

Quark Nuclear Physics with Heavy Quarks

Nora Brambilla *

Abstract Heavy quarks have been instrumental for progress in our exploration of strong interactions. Quarkonium in particular, a heavy quark-antiquark nonrelativistic bound state, has been at the root of several revolutions. Quarkonium is endowed with a pattern of separated energy scales qualifying it as special probe of complex environments. Its multiscale nature has made a description in Quantum Field Theory particularly difficult up to the advent of nonrelativistic effective field theories. We will focus on systems made by two or more heavy quarks. After considering some historical approaches based on the potential models and the Wilson loop approach, we will introduce the contemporary nonrelativistic effective field theory descriptions, in particular potential nonrelativistic QCD which entails the Schrödinger equation as zero order problem, define the potentials as matching coefficients and allows systematic calculations of the physical properties. The effective field theory allows us to explore quarkonium properties in the realm of QCD. In particular it allows us to make calculations with unprecedented precision when high order perturbative calculations are possible and to systematically factorize short from long range contributions where observables are sensitive to the nonperturbative dynamics of QCD. Such effective field theory treatment can be extended at finite temperature and in presence of gluonic and light quark excitations. We will show that in this novel theoretical framework, quarkonium can play a crucial role for a number of problems at the frontier of our research, from the investigation of the confinement dynamics in strong interactions to the study of deconfinement and the phase diagram of nuclear matter, to the precise determination of Standard Model parameters up to the emergence of exotics X Y Z states of an unprecedented nature.

Nora Brambilla

Physik-Department, Technische Universität München, James-Frank-Str. 1, 85748 Garching, Germany; Institute for Advanced Study, Technische Universität München, Lichtenbergstrasse 2 a, 85748 Garching, Germany; Munich Data Science Institute, Technische Universität München, Walther-von-Dyck-Strasse 10, 85748 Garching, Germany e-mail: nora.brambilla@ph.tum.de

* corresponding author

The role of heavy quarks

Heavy quarks and bound states of heavy quarks, primarily quarkonium, a bound state of a heavy quark and a heavy antiquark, have been historically instrumental to construct the theory of strong interactions and continue today to be at the forefront of our research as a golden probe of the strong dynamics.

The discovery of heavy quarks drastically changed the Standard Model (SM) of particle physics. This happened in the November revolution of 1974 when two labs on opposite sides of USA announced discovery of a new particle, a fact that helped the acceptance of the Standard Model of particle physics [1, 2]. The new particle was the first example of quarkonium: the J/ψ , the lowest excitation made by a charm and an anticharm. The J/ψ appeared as an unprecedented sharp peak, tall and narrow, 3 GeV in mass and 90 KeV in width, at variance with the typical width of several tens and hundreds of MeV of the hadrons discovered up to that time, i.e. strongly interacting light quark composite particles. The J/ψ discovery represented the confirmation of the quark model, the discovery of the charm quark, the confirmation of the GIM mechanism [4] (the mechanism through which flavour-changing neutral currents are suppressed in loop diagrams) and the first discovery of a quark of large mass moving nonrelativistically. It triggered additional searches and in few years the higher excitations of charmonium were discovered as well as bottomonia (1977), i.e. bound states of bottom and antibottom, B_c (1998), and the top (1995). States made by top and antitop decay weakly before forming a proper bound state, however still leaving their signature in the form of an enhancement of the cross section at threshold [28].

The J/ψ discovery was the confirmation of QuantumChromoDynamics (QCD) [3], the Quantum Field Theory describing strong interactions. QCD has a well defined behaviour in the ultraviolet (UV) region at large energy and a fundamental coupling constant $\alpha_s = g^2/4\pi$ running from small values at large energy to large values at small energy. This encodes the properties of asymptotic freedom (quarks are free at high momentum transfer) and confinement (quarks are confined in color singlet hadrons at low energy) [6]. As we will see, confinement becomes manifest in the case of heavy quarks, where one can write the color singlet quark-antiquark interaction potential in terms of a so called Wilson loop [13]. Confinement emerges in an area law of the Wilson loop and correspondingly in a linear potential growing with the distance between the quarks [8]. An emergent scale Λ_{QCD} parametrizes the importance of the nonperturbative corrections, i.e. the contributions that cannot be calculated in an expansion in α_s and is mirrored in the hadron spectrum, the mass of the proton being proportional to Λ_{QCD} . We consider a quark to be heavy when its mass m is larger than the scale Λ_{QCD} : this qualifies as heavy the charm, bottom and top quarks.

These fundamental features of QCD find the best realization in the J/ψ and in quarkonium in general. The small width can be explained by the fact that J/ψ is the lowest energy level and can decay only via annihilation, which makes available in the process a large energy, of order of two times the mass of the charm (about 2 GeV). The annihilation width is then proportional to $\alpha_s^2(2m_c)$ which is small due

to asymptotic freedom, since m_c is bigger than Λ_{QCD} . On the other hand, when theorists set up to investigate the structure of the energy levels of charmonium and bottomonium, they noticed that it can be reproduced by using in the Schrödinger equation a static potential superposition of an attractive Coulomb contribution (with the appropriate $SU(3)$ color factor for a singlet $Q\bar{Q}$) and a term linear in the distance: the famous Cornell potential [36, 37]. Such form of the potential has been later confirmed by nonperturbative calculations performed using computational lattice QCD [8, 13, 40, 42, 44]. In 1977 the static potential was calculated at two loops [5] which enabled to reobtain the QCD β function at order $O(g^5)$ and the solution of the Callan-Symanzik equation to order g^5 , which gave a hint on the existence of a color confining potential.

In the following we will address the importance of heavy quarks for quark nuclear physics. We will focus on systems made by two or more heavy quarks and discuss how they play a crucial role for a number of problems at the frontier of our research, from the investigation of the confinement dynamics in QCD to the study of deconfinement and the phase diagram of nuclear matter, to the precise determination of Standard Model parameters up to the emergence of exotics X Y Z states of an unprecedented nature [26, 28, 29, 30, 27]. In particular, we will conclude that our progress in these strong interactions topics is connected to a broad sweep of physical problems in settings ranging from astrophysics and cosmology to strongly correlated systems in particle and condensed matter physics as well as to search of physics beyond the Standard model.

Heavy quarks had and have a key role to address the phenomenon of CP (Charge Conjugation and Parity) violation, which is crucial to understand the asymmetry between matter and antimatter that exists in the Universe, by testing and constraining the Cabibbo-Kobayashi-Maskawa matrix entries entering B and D mesons decays and mixing and by identifying new physics contributions, see e.g. the reviews [19, 20, 21, 22]. The Babar and Belle experiments at the B factories [23, 24] have been constructed to this aim but turned out to be also formidable heavy mesons machines giving a great boost to our knowledge of heavy quark systems and their strong interaction dynamics.

The review is organized as follows. First, we will discuss the physics characteristics of systems made by heavy quarks. Then, we will summarize what have been historically the pioneering approaches and the phenomenological models. After that, we will explain that to address in quantum field theory a nonrelativistic multiscale system like quarkonium, it is necessary resort to nonrelativistic effective field theories (NREFTs). We will show how to construct NREFTs up to arriving at the simplest possible version, called potential nonrelativistic QCD (pNRQCD) which implements the Schrödinger equation as the zero order problem. Then, we will show how combining NREFTs and lattice we can get systematic and under control predictions on a number of physical processes and observables like the spectrum, decays, transitions and production. In this framework quarkonium becomes a unique laboratory for the study of strong interactions from the high energy to the low energy scales. The NREFT allows us to explore quarkonium properties in the realm of QCD. In particular it allows us to make calculations with unprecedented

precision when high order perturbative calculations are possible and to systematically factorize short from range contributions where observables are sensitive to the nonperturbative dynamics of QCD. Finally, we will address some of the most interesting open problems in relation to quarkonium, i.e. the non-equilibrium propagation of quarkonium in medium which calls for introducing open quantum system on top of NREFTs and the new exotic states X Y Z discovered at the accelerator experiments.

Heavy-light mesons, quarkonia , baryons with two or more heavy quarks

Heavy quarkonia are systems composed by a heavy quark and a heavy antiquark with mass m larger than the “QCD confinement scale” Λ_{QCD} , so that $\alpha_s(m) \ll 1$ holds. We have that $m_c \sim 1.5$ GeV and $m_b \sim 5$ GeV. Of course the quark masses are scheme dependent objects and their actual value depends on the considered scheme and scale, only the pole mass being scale independent, see e.g. the review [47]. From the quarkonia spectra, see Fig. 1 (and 2 and 3), it is evident that the difference in the orbital energy levels is much smaller than the quark mass. It scales like mv^2 , while fine and hyperfine separations scale like mv^4 . Here v is the heavy quark velocity ($v = |\mathbf{v}|$) in the rest frame of the meson in units of c , and $v^2 \sim 0.1$ for the $b\bar{b}$, $v^2 \sim 0.3$ for $c\bar{c}$ systems. This is the same scaling of the hydrogen atom if one identifies v with the fine structure constant α_{em} . Therefore quarkonia are nonrelativistic systems. Being nonrelativistic, quarkonia are characterized by a hierarchy of energy scales: the mass m of the heavy quark (hard scale), the typical relative momentum $p \sim mv$ (in the meson rest frame) corresponding to the inverse Bohr radius $r \sim 1/(mv)$ (soft scale), and the typical binding energy $E \sim mv^2$ (ultrasoft scale). Of course, for quarkonium there is another scale that can never be switched off in QCD, i.e. Λ_{QCD} , the scale at which non perturbative effects become dominant. A similar pattern of scales emerge in the case of baryons composed of two or three heavy quarks [96] and for the just discovered state $X(6900)$ [38] made by two charm and two anticharm quarks. The pattern of nonrelativistic scales makes all the difference between heavy quarkonia and heavy-light mesons, which are characterized by just two scales: m and Λ_{QCD} .

Being a multiscale system, heavy quarkonium is probing different energy regimes of the strong interactions, from the hard region, where an expansion in the coupling constant is possible and precision studies may be done, to the low-energy region, dominated by confinement and the many manifestations of nonperturbative dynamics. In addition, the properties of production and absorption of quarkonium in a nuclear and hot medium are crucial inputs for the study of QCD at high density and temperature, reaching out to cosmology. On the experimental side the diversity, quantity and accuracy of the data collected in the last decades is impressive and includes clean and precise samples of quarkonia spectra decay, transition and production processes, including the discovery of exotics X Y Z states at tau-charm (BES experiment) and B factories (Babar and Belle experiments), hadroproduction

at Fermilab Tevatron and the Large Hadron Collider (LHC) experiments at CERN, production in photon-gluon fusion at DESY, photoproduction at Jlab, heavy ions production and suppression at RHIC, NA60, and LHC. New data are coming also from the upgraded experiments BELLE II and BESIII [26, 28, 29, 30, 33] and more will come in future from Panda at FAIR and the Electron Ion Collider (EIC) [33, 35]. On the theoretical side the last few decades have seen the construction of new non-relativistic effective field theories and new development in computational lattice QCD which supply us with a systematic calculational framework in quantum field theory. All this make quarkonium a golden probe of strong interactions.

From now on we will concentrate on the study of systems with two or more heavy quarks. We will outline the rich interplay of theoretical advancement and experimental success and its implication on our control of strong interactions inside the Standard Model of Particle Physics. Before, however, I will summarize the models that have been used in the past to describe the quarkonium properties.

The potential and the phenomenology of quarkonium

You find in Figs. (2) and (3) our present knowledge about the states in the charmonium and in the bottomonium sector. We will consider in the following quarks of equal mass for simplicity (in the case of B_c one should take into account that the masses are different). The quark and the antiquark spins combine to give the total spin $\mathbf{S} = \mathbf{S}_1 + \mathbf{S}_2$ which combines with the orbital angular momentum \mathbf{L} to give the total angular momentum \mathbf{J} . The resulting state solution of a Schrödinger equation is denoted by $n^{2S+1}L_J$ where $n - 1$ is the number of radial nodes of the wave function. As usual, to $L = 0$ is given the name S , to $L = 1$ the name P , to $L = 2$ the name D and so on. The experimental resonances (see Figs. (2) and (3)) are classified via the J^{PC} quantum numbers, $P = (-1)^{L+1}$ being the parity number and $C = (-1)^{L+S}$ the C-parity. Strong decay thresholds are marked by horizontal dashed lines that represent the energy necessary to decay in a couple of heavy-light mesons. In the charmonium sector only 10 states of the states presented in Fig. (2) have been discovered before 1980 and no one between 1980 and 2002. In 2003 the new revolution started with the discovery of the $X(3872)$ [125] and a number of new states above and below the strong decay threshold [26]. Many of the states discovered at or above threshold presented exotic features and have been initially termed X Y Z states [123].

The first tool used to describe quarkonium in the eighties has been the quark model with some notions of QCD incorporated. In particular, constituent heavy quark masses have been considered and a static potential called Cornell potential [36, 37] has been used in a Schrödinger equation, successfully reproducing the quarkonia levels measured at that time. The Cornell potential is flavor independent and has the form

$$V_0(r) = -\frac{\kappa}{r} + \sigma r + \text{const}, \quad (1)$$

r being the modulus of the quark-antiquark distance. The parameters κ should be identified with $\frac{4}{3}\alpha_s$, corresponding to the one gluon exchange that should dominate at small distances due to asymptotic freedom, and the string tension σ corresponds to a constant energy density related to confinement and originating a potential growing with the interquark distance at large distances. A fit to the states gave $\kappa = 0.52$ and $\sigma = 0.182 \text{ GeV}^2$. Since then, several different phenomenological forms of the static potential have been exploited, see [14, 13] for a review. In order to explain the fine and hyperfine structure of the quarkonium spectrum, however, spin dependent relativistic corrections to the static potential have to be considered. Moreover, for $v^2 \sim 0.1$ for the $b\bar{b}$, $v^2 \sim 0.3$ for $c\bar{c}$ systems, one expects relativistic corrections of order $20 \div 30\%$ for the charmonium spectrum and up to 10% for the bottomonium spectrum and also spin independent but momentum dependent corrections have to be considered, arriving at a phenomenological hamiltonian of the type

$$H = \sum_{j=1,2} \left(m_j + \frac{p_j^2}{2m_j} - \frac{p_j^4}{8m_j^3} \right) + V_0 + V_{\text{SD}} + V_{\text{VD}}. \quad (2)$$

The $1/m^2$ spin-dependent V_{SD} and velocity-dependent V_{VD} potentials were initially derived in the eighties from the semirelativistic reduction of a Bethe–Salpeter (BS) [16] equation for the quark-antiquark connected amputated Green functions or, equivalently at this level, from the semirelativistic reduction of the quark-antiquark scattering amplitude with an effective exchange equal to the BS kernel. Several ambiguities are involved in this procedure, due on one hand to the fact that we do not know the relevant confining nonperturbative Bethe–Salpeter kernel, on the other hand due to the fact that we have to get rid of the temporal (or energy Q_0 , $Q = p_1 - p'_1$ being the momentum transfer) dependence of the kernel to recover a potential (instantaneous) description. It turned out that, at the level of the approximation involved, the spin-independent relativistic corrections at the order $1/m^2$ depend on the way in which Q_0 is fixed together with the gauge choice of the kernel [17, 14, 13]. The Lorentz structure of the kernel was also not known. On a phenomenological basis, the following ansatz for the kernel was intensively studied [13]

$$I(Q^2) = (2\pi)^3 [\gamma_1^\mu \gamma_2^\nu P_{\mu\nu} J_\nu(Q) + J_s(Q)] \quad (3)$$

in the instantaneous approximation $Q_0 = 0$.

Notice that the effective kernel above was taken with a pure dependence on the momentum transfer Q . But, of course, the dependence on the quark and antiquark momenta could have been more complicated. The vector kernel $J_\nu(Q)$ above would correspond to the one gluon exchange (with $P_{\mu\nu}$ depending on the adopted gauge) while the scalar kernel $J_s(Q)$ would account for the nonperturbative interaction. Taking $J_\nu = -\frac{1}{2\pi^2} \frac{4}{3} \frac{1}{Q^2}$ and $J_s = -\frac{\sigma}{\pi^2} \frac{1}{Q^4}$, reproduce the Cornell potential and the corrections in the nonrelativistic reduction of such kernel in the instantaneous approximation would give a form for the V_{SD} and the V_{VD} . The confining part of the

kernel was usually chosen to be a Lorentz scalar in order to match the data on the fine separation on the P states [18]. If one however takes a kernel which is not a pure convolution kernel, as it is to be expected in interactions generated at higher orders, and deals more appropriately with the instantaneous approximation, one can get quite different relativistic corrections, especially for the velocity dependent part [17]. We conclude that this type of description is model dependent and does not allow for further progress. In particular, the parameters of the model cannot be related to the underlying field theory and the systematics of the model cannot be estimated.

A more systematic procedure to relate the potential to QCD has been based on the so called Wilson loop approach. In order to obtain information on the structure of nonperturbative corrections to the potential it is useful to define the potential in terms of gauge invariant objects suitable for a direct lattice QCD evaluation. Indeed lattice QCD is one of the best methods to extract nonperturbative information from QCD, for some reviews see [39, 40, 41, 42, 43]. Let us see how this works in the case of the static potential. Let us consider a locally gauge invariant quark-antiquark color singlet state (for more details see [13, 14]:

$$|\phi_{\alpha\beta}^{lj}\rangle \equiv \frac{\delta_{lj}}{\sqrt{3}} \bar{\psi}_{\alpha}^j(x) U^{ik}(x, y, C) \psi_{\beta}^k(y) |0\rangle \quad (4)$$

where i, j, k, l are colour indices (that will be suppressed in the following), $|0\rangle$ denotes the QCD ground state and the Schwinger string line has the form

$$U(x, y; C) = P \exp \left\{ ig \int_y^x A_{\mu}(z) dz^{\mu} \right\}, \quad (5)$$

where $A_{\mu} = A_{\mu}^a$, $a = 1, 8$ is the gluon vector potential of QCD in the fundamental representation, g the QCD coupling constant, and the integral is extended along the path C . The operator P denotes the path-ordering prescription which is necessary due to the fact that A_{μ} are non-commuting matrices. Let us see how the quark-antiquark potential can be extracted from the quark-antiquark Green function constructed with such color singlet states:

$$G(T) = \langle \phi(\mathbf{x}, 0) | \phi(\mathbf{y}, T) \rangle = \langle \phi(\mathbf{x}, 0) | \exp(-iHT) | \phi(\mathbf{y}, 0) \rangle. \quad (6)$$

Inserting a complete set of energy eigenstates ψ_n with eigenvalues E_n and making a Wick rotation we find

$$\begin{aligned} G(-iT) &= \sum_n \langle \phi(\mathbf{x}, 0) | \psi_n \rangle \langle \psi_n | \phi(\mathbf{y}, 0) \rangle \exp(-E_n T) \\ &\rightarrow \langle \phi(\mathbf{x}, 0) | \psi_0 \rangle \langle \psi_0 | \phi(\mathbf{y}, 0) \rangle \exp(-E_0 T) \quad \text{for } T \rightarrow \infty \end{aligned} \quad (7)$$

which gives the Feynman–Kac formula for the ground state energy

$$E_0 = - \lim_{T \rightarrow \infty} \frac{\log G(-iT)}{T}. \quad (8)$$

The only condition for the validity of Eq. (8) is that the ϕ states have a non-vanishing component over the ground state. This is precisely the way in which hadron masses are computed on the lattice. Of course, to maximize the overlap with the ground state in consideration appropriate operators may be used. If the ϕ state denotes a state of two exactly static particles interacting at a distance r , then the ground state energy is a function of the particle separation, $E_0 \equiv E_0(r)$, and gives the potential of the first adiabatic surface. It is possible to obtain an explicit analytic form of the quark-antiquark Green function for infinitely heavy quarks ($m \rightarrow \infty$, static limit) and for large temporal intervals ($T \rightarrow \infty$), see [13]. We consider that at a time $t = 0$ a quark and an antiquark pair is created and that they interact while propagating for a time $t = T$ at which they are annihilated. Then $(x_j = (\mathbf{x}_j, T), y_j = (\mathbf{y}_j, 0))$, see Fig. 4) we obtain

$$G_{\beta_1\beta_2\alpha_1\alpha_2}(T) \xrightarrow{m \rightarrow \infty} \delta^3(\mathbf{x}_1 - \mathbf{y}_1) \delta^3(\mathbf{x}_2 - \mathbf{y}_2) (P_+)_{\beta_1\alpha_1} (P_-)_{\alpha_2\beta_2} \times e^{-2mT} \langle \text{Tr} P e^{ig \oint_{I_0} dz_\mu A_\mu(z)} \rangle \quad (9)$$

with $P_\pm \equiv (1 \pm \gamma_4)/2$. The integral in Eq. (9) extends over the circuit I_0 which is a closed rectangular path with spatial and temporal extension $r = |\mathbf{x}_1 - \mathbf{x}_2|$ and T respectively, and has been formed by the combination of the path-ordered exponentials along the horizontal (=time fixed) lines, coming from the Schwinger strings, and those along the vertical lines coming from the static propagators (see Fig. 4). The brackets in (9) denote the QCD vacuum expectation value, which in Euclidean space is

$$\langle f[A] \rangle \equiv \frac{1}{Z} \int \mathcal{D}A f[A] e^{-\int d^4x L_M^E}. \quad (10)$$

From Eq. (9) it is clear that the dynamics of the quark-antiquark interaction is contained in

$$W(I_0) = \text{Tr} P e^{ig \oint_{I_0} dz_\mu A_\mu(z)}. \quad (11)$$

This is the famous static Wilson loop [6]. In the limit of infinite quark mass considered, the kinetic energies of the quarks drop out of the theory, the quark Hamiltonian becomes identical with the potential while the full Hamiltonian contains also all types of gluonic excitations. According to the Feynman–Kac formula the limit $T \rightarrow \infty$ projects out the lowest state i.e. the one with the “glue” in the ground state. This has the role of the quark-antiquark potential for pure mesonic states. We will see in the section over exotics that the excited states have the role of the potential in the case of hybrid states, i.e. states with gluons contributing to the binding. Now, comparing Eq. (9) with Eq. (7) and considering that the exponential factor $\exp(-2mT)$ just accounts for the fact that the energy of the quark-antiquark system includes the rest mass of the pair, we obtain

$$V_0(r) \equiv E_0(r) = - \lim_{T \rightarrow \infty} \frac{1}{T} \log \langle W(I_0) \rangle. \quad (12)$$

The heavy quark degrees of freedom have now completely disappeared and the expectation value in (12) can be evaluated in the pure Yang–Mills theory or in unquenched QCD (i.e. taking into account sea light quarks) [6, 7]. Notice that the potential is given purely in terms of a gauge invariant quantity (the Wilson loop precisely). In this way we have reduced the calculation of the static potential to a well posed problem in field theory: to obtain the actual form of V_0 we need to calculate the QCD expectation value of the static Wilson loop. The static Wilson loop is the low energy domain of QCD is dominated by an area law, i.e. can be approximated at leading order at large r as $\langle W(I_0) \rangle \sim \exp\{-\sigma r T\}$ (i.e. the area of the loop in the exponent multiplied by the string tension), as shown in the strong coupling expansion [40, 8, 42, 13, 9]. In the high energy domain the first perturbative contribution comes from the one gluon exchange and therefore Eq. (12) would reproduce in these limits the Cornell potential of Eq. (1), which appears to be a simple superposition of these two behaviours. We will come back to the area law behaviour of the Wilson loop in the section on studies of confinement. The Wilson loop formalism have been used to obtain the form of spin dependent V_{SD} potential in the famous papers of Eichten, Feinberg [48] and Gromes [49] and later to obtain the form of spin independent, momentum dependent V_{VD} potential in the classical works [50, 51]. These works express the relativistic corrections to the potential in terms of generalized static Wilson loops containing field strengths (i.e. chromoelectric and chromomagnetic fields) insertion in the quark lines. In [52] a nonstatic Wilson loop has been used to obtain the relativistic corrections to the static three-quarks potential.

Up to the establishment of the NREFT called potential nonrelativistic QCD in the nineties [59, 60, 47], the Wilson loop approach has been the best theory founded method and was used to calculate the potentials on the lattice (see e.g. the review [42]).

However, this method was providing only part of the QCD result. The Wilson loop relativistic potential corrections were missing all the non analytic term in the mass, $\ln m/\mu$ terms, that were instead obtained in a direct purely perturbative QCD one loop calculation [11]. Moreover, QCD in the static quark antiquark configuration can still change colour by emission of gluons. This introduces a new dynamical scale in the evaluation of the potential that should be taken into account as it became evident in the seminal paper of Appelquist Dine and Muzinich [12] that identified infrared divergences in the three loops perturbative fixed order calculation of the static Wilson. Moreover, already in [14] the question was raised about why potential models were working so well. It took a while and the development of non relativistic effective field theories to answer this question and to be able to calculate systematically the potentials from QCD.

All these problems are addressed and solved in pNRQCD.

Nonrelativistic effective field theories

As we mentioned, the study of quarkonium in the last few decades has witnessed two major developments: the establishment of nonrelativistic effective field theories (NREFTs) and progress in lattice QCD calculations of excited states and resonances, with calculations at physical light-quark masses. Both allow for precise and systematically improvable computations that are largely model-independent. It is precisely this advancement in the understanding of quarkonium and quarkonium-like systems inside QCD that makes today quarkonium exotics as particularly valuable (see the section on Exotics). In fact, today that we are confronted with a huge amount of high-quality data, which have provided for the first time uncontroversial evidence for the existence of exotic hadrons, by using modern theoretical tools that allow us to explore in a controlled way these new forms of matter we can get a unique insight into the low-energy dynamics of QCD.

The appearance of a hierarchy of scales calls for the application of effective field theory (EFT) methods. However, “heavy quark effective theory” (HQET) [45, 46], the EFT description of heavy-light mesons, where only an ultraviolet mass scale m and an infrared mass scale Λ_{QCD} appear, is not suitable for the description of heavy quarkonia, since HQET is unable to describe the dynamics of the binding. The existence of several physical scales makes the theoretical description of quarkonium physics more complicated. All scales get entangled in a typical amplitude involving a quarkonium observable. For example, quarkonium annihilation and production take place at the scale m , quarkonium binding takes place at the scale mv , which is the typical momentum exchanged inside the bound state, while very low-energy gluons and light quarks (also called ultrasoft (US) degrees of freedom) live long enough that a bound state has time to form and, therefore, are sensitive to the scale mv^2 . Ultrasoft gluons are responsible for phenomena similar to the Lamb shift in hydrogen atom. This pattern of scales has made the description in Quantum Field Theory particularly difficult. The solution is to take advantage of the existence of the different energy scales to substitute QCD with simpler but equivalent NREFTs. A hierarchy of NREFTs, see Fig.5, may be constructed by systematically integrating out modes associated with high-energy scales not relevant for the quarkonium system. Such integration is made in a matching procedure that enforces the equivalence between QCD and the EFT at a given order of the expansion in v . The EFT Lagrangian is factorized in matching coefficients, encoding the high energy degrees of freedom and low energy operators. The relativistic invariance is realized via exact relations among the matching coefficients [64, 65, 66, 67] The EFT displays a power counting in the small parameter v , therefore we are able to attach a definite power of v to the contribution of each EFT operators to the physical observables. We will introduce in the next sections nonrelativistic QCD (NRQCD) [53, 54, 55] and potential nonrelativistic QCD (pNRQCD) [58, 60], see the review [47].

It turns to be instrumental to combine NREFTs and lattice. In fact, on one hand, the NREFT is pulling out scales from observables in a controlled way, separating them, and delivering results for calculations at large scales including the logs resummation. On the other hand, the low energy contributions that the EFT has factorized

are often nonperturbative and can be evaluated on the lattice. This greatly reduces the complexity of the problem allowing the lattice to target the nonperturbative part directly, appropriately defined in the EFT in terms of gauge invariant, purely gluonic objects, a big simplification with respect to an ab initio lattice calculation of an observable. The latter is much more difficult because still contains all the physical scales of the problem. In this framework also quenched lattice calculations can be pretty useful because at least at higher energy the flavor dependence is accounted for by the EFT matching coefficients. We founded the TUMQCD lattice collaboration precisely to address these calculations directly inside the EFT [61].

Nonrelativistic QCD

Nonrelativistic QCD (NRQCD) [54, 53], follows from QCD integrating out the scale m . As a consequence, the effective Lagrangian is organized as an expansion in $1/m$ and $\alpha_s(m)$:

$$\mathcal{L}_{\text{NRQCD}} = \sum_n \frac{c_n(\alpha_s(m), \mu)}{m^n} \times O_n(\mu, mv, mv^2, \dots), \quad (13)$$

where c_n are Wilson coefficients that contain the contributions from the scale m . They can be calculated via a well defined procedure call matching, see e.g. [47], in which one calculates in perturbation theory Green Functions or amplitudes in QCD and in NRQCD, expand in $1/m$ and insert the difference between the two calculations (i.e. the non analytic terms in the scale that is been integrated out, the mass) inside the matching coefficients of the EFT. In fact since in NRQCD we expand in the mass no contributions of the form $\log(m/\mu)$ can be generated in calculations in the EFT.

The O_n are local operators of NRQCD; the matrix elements of these operators contain the physics of scales below m , in particular of the scales mv and mv^2 and also of the nonperturbative scale Λ_{QCD} . Finally, the parameter μ is the NRQCD factorization scale. The low-energy operators O_n are constructed out of two or four heavy quark/antiquark fields plus gluons. At the lowest order in the $1/m$ expansion the NRQCD Lagrangian density is

$$\begin{aligned} \mathcal{L}_{\text{NRQCD}} = & \psi^\dagger \left\{ iD^0 + \frac{\mathbf{D}^2}{2m} \right\} \psi + \chi^\dagger \left\{ iD^0 - \frac{\mathbf{D}^2}{2m} \right\} \chi \\ & - \frac{1}{4} F_{\mu\nu}^a F^{\mu\nu a}, \end{aligned} \quad (14)$$

where ψ is the Pauli spinor field that annihilates the fermion and χ is the Pauli spinor field that creates the antifermion; $iD^0 = i\partial_0 - gA^0$ and $i\mathbf{D} = i\nabla + g\mathbf{A}$. At order $1/m^2$ bilinear terms in the quark (antiquark) field containing the chromoelectric and chromomagnetic fields, as well covariant derivatives and so on start to appear. These are of the same form that one would obtain from a Foldy-Wouthuysen

transformation but in addition are multiplied by matching coefficients that contain the UV behaviour of QCD. In addition, four fermion terms start to appear at order $1/m^2$ with matching coefficients containing both real and imaginary parts. The presence of imaginary parts describe the decays of quarkonium via annihilation of hard gluons that have been integrated out from the theory.

The quarkonium state $|H\rangle$ in NRQCD is expanded in the number of partons

$$|H\rangle = |\bar{Q}Q\rangle + |\bar{Q}Qg\rangle + |\bar{Q}Q\bar{q}q\rangle + \dots \quad (15)$$

where the states including one or more light parton are shown to be suppressed by powers of v . In the $|\bar{Q}Qg\rangle$ for example the quark-antiquark are in a color octet state. The NRQCD lagrangian has been extensively used on the lattice to calculate quarkonium spectra and decays. On the other hand, NRQCD has been deeply impactful on the study of quarkonium production at the LHC putting forward a factorization formula for the inclusive cross section for the direct production of the quarkonium H at large transverse momentum written as a sum of products of NRQCD matrix elements and short-distance coefficients:

$$\sigma[H] = \sum_n \sigma_n \langle \mathcal{K}_n^{4\text{fermions}} \rangle \quad (16)$$

where the σ_n are short-distance coefficients, and the matrix elements $\langle \mathcal{K}_n^{4\text{fermions}} \rangle$ are vacuum-expectation values containing four-fermions operators in color singlet and color octet configurations identified by $Q\bar{Q}$ angular momentum state quantum numbers. They contain in the middle a projector over the $Q\bar{Q}$ pair plus anything and some Schwinger lines with a particular path to make them gauge invariant. The factorization for production is proved only at order NNLO and in some cases [56, 57]. It is different from the NRQCD factorization of inclusive decays that is proven at all orders. In such case the low energy part contains quarkonium expectation values of color singlet and color octet four quark operators without the projector in the middle. The matrix elements (LDMEs, long distance matrix elements) $\langle \mathcal{K}_n^{4\text{fermions}} \rangle$ contain all of the nonperturbative physics associated with the evolution of the $Q\bar{Q}$ pair into a quarkonium state and they are universal. Their NRQCD definition does not allow a lattice calculation and their extractions from collider data is still challenging [26, 30, 29, 31, 32]. Differently from HQET, the power counting of NRQCD is not unique, due to the fact that many physical scales are still dynamical ($mv, mv^2, \Lambda_{\text{QCD}}$). This still complicates bound state calculations as the soft and US scale can get entangled.

potential Nonrelativistic QCD

Quarkonium formation happens at the scale mv . The suitable NREFT is potential Nonrelativistic QCD, pNRQCD [58, 60, 47], which follows from NRQCD by integrating out the scale $mv \sim r^{-1}$. The pNRQCD description directly addresses the

bound state dynamics, implements the Schrödinger equation as zero order problem, properly defines the potentials as matching coefficients, and allows to systematically calculate relativistic and retardation corrections. In this way even quantum mechanics can also be reinterpreted as a pNREFT. Moreover, since the scale mv has been integrated out, the power counting of pNRQCD is less ambiguous than the one of NRQCD.

The soft scale, proportional to the inverse quarkonium radius r , may be either perturbative ($mv \gg \Lambda_{\text{QCD}}$) or nonperturbative ($mv \sim \Lambda_{\text{QCD}}$) depending on the physical system under consideration. We do not have any direct information on the radius of the quarkonia, and thus the attribution of some of the lowest bottomonia and charmonia states to the perturbative or the nonperturbative soft regime may be ambiguous, but it is likely that the lowest bottomonium and possibly also the lowest charmonium states have small enough radii that the scale mv is in fact still perturbative. In a case with $\Lambda_{\text{QCD}} \ll mv^2$ both scales are still perturbative and the system would be similar to a Coulombic system. For such a quarkonium we would have - similar as for the hydrogen atom - $v \sim \alpha_s(mv)$. However, none of the $b\bar{b}$ and $c\bar{c}$ states satisfy this condition. In all realistic quarkonia ($b\bar{b}$ and $c\bar{c}$) the ultrasoft scale is nonperturbative. Only for $t\bar{t}$ threshold states the ultrasoft scale may be considered still perturbative. In Fig. 5 we schematically show the various scales. The short-range quarkonia are small enough to allow for a perturbative treatment of the scale mv , while for the long range quarkonia already this scale requires a non perturbative treatment.

In the next section we will present weakly coupled and strongly coupled pNRQCD, discuss the form of the potential and briefly address the countless phenomenological applications of this that has become the standard treatment for quarkonium. On one hand, pNRQCD allows us systematic and precise determinations of processes at high energy collider experiments and the definition and computation of quantities of large phenomenological interest, on the other hand the systematic factorization enables us for studies of confinement. The low energy nonperturbative factorized effects depend on the size of the physical system: when Λ_{QCD} is comparable or smaller than mv they are carried by correlators of chromoelectric or chromomagnetic fields nonocal or local in time, when Λ_{QCD} is of order mv they are carried by generalized static Wilson loops, non local in space, with insertion on chromoelectric and chromomagnetic fields. The EFT allows us to make model independent predictions and we can use the power counting to attach an error to the theoretical predictions. The nonperturbative physics in pNRQCD is encoded in few low energy correlators that depend only on the glue and are gauge invariant: these are objects in principle ideal for lattice calculations. Even more interesting is that this EFT description allows modifications to be used to describe exotics states (BOEFT) and the nonequilibrium evolution of quarkonium in medium (pNRQCD at finite temperature with open quantum system) as we will address in the last two sections.

Weakly coupled pNRQCD

When $mv \gg \Lambda_{\text{QCD}}$, we speak about weakly-coupled pNRQCD because the soft scale is perturbative and the matching from NRQCD to pNRQCD may be performed in perturbation theory. The lowest levels of quarkonium, like J/ψ , $\Upsilon(1S)$, $\Upsilon(2S) \dots$, may be described by weakly coupled pNRQCD, while the radii of the excited states are larger and presumably need to be described by strongly coupled pNRQCD. All this is valid for states away from strong-decay threshold, i.e. the threshold for a decay into two heavy-light hadrons. The effective Lagrangian is organized as an expansion in $1/m$ and $\alpha_s(m)$, inherited from NRQCD, and an expansion in r (multipole expansion) [60, 47]

$$L_{\text{pNRQCD}}^{\text{weak}} = \int d^3R \int d^3r \sum_n \sum_k \frac{c_n(\alpha_s(m), \mu)}{m^n} V_{n,k}(r, \mu', \mu) r^k \times O_k(\mu', mv^2, \dots), \quad (17)$$

where \mathbf{R} is the center of mass position and O_k are the operators of pNRQCD. We do not show explicitly the part of the lagrangian involving gluons and light quarks, as this part coincides with the QCD one. The matrix elements of the operators above depend on the low-energy scale mv^2 and μ' , where μ' is the pNRQCD factorization scale. The $V_{n,k}$ are the Wilson coefficients of pNRQCD that encode the contributions from the scale r and are nonanalytic in r . The c_n are the NRQCD matching coefficients as given in (13).

The degrees of freedom, which are relevant below the soft scale, and which appear in the operators O_k , are $Q\bar{Q}$ states (a color-singlet S and a color-octet $O = O_a T^a$ state, depending on \mathbf{r} and \mathbf{R}) and (ultrasoft) gluon fields, which are expanded in r as well (multipole expanded and depending only on \mathbf{R}). pNRQCD makes apparent that the correct zero order problem is the Schrödinger equation. Looking at the equations of motion of pNRQCD, we may identify $V_{n,0} = V_n$ with the $1/m^n$ potentials that enter the Schrödinger equation and $V_{n,k \neq 0}$ with the couplings of the ultrasoft degrees of freedom, which provide corrections to the Schrödinger equation. These nonpotential interactions, associated with the propagation of low-energy degrees of freedom start to contribute at NLO in the multipole expansion. They are typically related to nonperturbative effects and are carried by purely gluonic correlator local or nonlocal in time: they need to be calculated on the lattice.

In particular at the NLO in the multipole expansion at leading order in the expansion in $1/m$, the pNRQCD Lagrangian density is

$$\begin{aligned} \mathcal{L}_{\text{pNRQCD}}^{\text{weak}} = & \text{Tr} \left\{ S^\dagger \left(i\partial_0 - \frac{\mathbf{p}^2}{m} - V_s(r) + \dots \right) S \right. \\ & \left. + O^\dagger \left(iD_0 - \frac{\mathbf{p}^2}{m} - V_o(r) + \dots \right) O \right\} \\ & + gV_A(r) \text{Tr} \{ O^\dagger \mathbf{r} \cdot \mathbf{E} S + S^\dagger \mathbf{r} \cdot \mathbf{E} O \} + g \frac{V_B(r)}{2} \text{Tr} \{ O^\dagger \mathbf{r} \cdot \mathbf{E} O + O^\dagger O \mathbf{r} \cdot \mathbf{E} \}, \end{aligned} \quad (18)$$

where $\mathbf{R} \equiv (\mathbf{x}_1 + \mathbf{x}_2)/2$, $S = S(\mathbf{r}, \mathbf{R}, t)$ and $O = O(\mathbf{r}, \mathbf{R}, t)$ are the singlet and octet quark-antiquark composite nonrelativistic fields respectively. All the gauge fields in Eq. (19) are evaluated in \mathbf{R} and t . In particular $\mathbf{E} \equiv \mathbf{E}(\mathbf{R}, t)$ and $iD_0 O \equiv i\partial_0 O - g[A_0(\mathbf{R}, t), O]$. V_s^0 and V_o^0 are the singlet and octet heavy $Q\bar{Q}$ static potentials. Higher-order potentials in the $1/m$ expansion and the centre-of-mass kinetic term are not shown here and are indicated by the dots. At higher order in the multipole expansion and in the $1/m$ expansion more operators appears containing US chromomagnetic and chromoelectric fields but they are suppressed in the power counting in v . We define

$$\begin{aligned} V_s^0(r) &\equiv -C_F \frac{\alpha_{V_s}(r)}{r}, \\ V_o^0(r) &\equiv \left(\frac{C_A}{2} - C_F \right) \frac{\alpha_{V_o}(r)}{r} \end{aligned} \quad (19)$$

which shows that the singlet potential is attractive and the octet one is repulsive. V_A and V_B are the matching coefficients associated in the Lagrangian (19) to the leading corrections in the multipole expansion. Both the potentials and the coefficients V_A and V_B have to be determined by matching pNRQCD with NRQCD at a scale μ smaller than $m v$ and larger than the US scales. Since, in particular, μ is larger than Λ_{QCD} the matching can be done perturbatively. At the lowest order in the coupling constant we get $\alpha_{V_s} = \alpha_{V_o} = \alpha_s$, $V_A = V_B = 1$. In order to have the proper free-field normalization in the colour space we define

$$S \equiv \frac{\mathbb{1}_c}{\sqrt{N_c}} S \quad O \equiv \frac{T^a}{\sqrt{T_F}} O^a, \quad (20)$$

where $T_F = 1/2, N_c = 3$.

The perturbative QCD potential

For system with a perturbative soft scale the potentials can be calculated in perturbation theory, i.e. no nonperturbative quantities enter the potential [47]. The potentials can be calculated at all order in the perturbative expansion in α_s via a well defined matching procedure that entails to compare appropriate Green functions in NRQCD and in pNRQCD calculated in perturbation theory up to the desired order of the perturbative expansion, order by order in $1/m$ and order by order in the multipole expansion. The difference between the two is encoded in the matching coefficients. On the pNRCD side lower energy scales may be expanded in the loop integral and give no contribution in the matching in dimensional regularization. The singlet static potential is calculated by matching the relevant NRQCD green function (the static Wilson loop) and the pNRQCD singlet Green function see Fig. 6). At three loops, an ultrasoft (US) divergence is emerging at fixed order calculation that can be regularized resumming series of diagrams containing the US scale which is the difference between the singlet and the octet potential, see [59, 47].

This solves the problem raised by Appelquist Dine and Muzinich [12], it explains how this divergence cancels between the potential ($\log r \mu$) and the contribution of the US chromoelectric correlator $\log((V_o - V_s)/\mu)$ (second contribution in the r.h. s.

of Fig. (6)) leaving a term in $\log \alpha_s$ in the static energy and qualifies the potential as a matching coefficient of an EFT which is depending on the US scale. Being matching coefficients of the effective field theory, the potentials undergo renormalization, develop a scale dependence and satisfy renormalization group equations, which allow to resum large US logarithms see e.g. [68, 69, 70].

In particular one obtains the complete expression for the static potential, at 3 loops, up to the relative order $\alpha_s^3 \ln \mu r$ in coordinate space (α_s is in the $\overline{\text{MS}}$ scheme) as:

$$\alpha_{V_s}(r, \mu) = \alpha_s(r) \left\{ 1 + (a_1 + 2\gamma_E \beta_0) \frac{\alpha_s(r)}{4\pi} \right. \quad (21)$$

$$\left. + \left[\gamma_E (4a_1 \beta_0 + 2\beta_1) + \left(\frac{\pi^2}{3} + 4\gamma_E^2 \right) \beta_0^2 + a_2 \right] \frac{\alpha_s^2(r)}{16\pi^2} + \frac{C_A^3}{12} \frac{\alpha_s^3(r)}{\pi} \ln r \mu \right\},$$

where β_n are the coefficients of the beta function, a_1 and a_2 are the constants at 1 and 2 loops respectively. We emphasize that this US contribution to the static potential would be zero in QED. From Eq. (22) is clear that α_{V_s} depends on the US scale and as such is not a short distance quantity.

The evaluated terms clarify the long-standing issue of how the perturbative static potential should be defined at higher order in the perturbative series. In perturbation theory the static potential does not coincide with the static Wilson loop starting from three loops. It should be emphasized that the separation between soft and US contributions is not an artificial trick but a necessary procedure if one wants to use the static potential in a Schrödinger-like equation in order to study the dynamics of $Q\bar{Q}$ states of large but finite mass. In that equation the kinetic term of the $Q\bar{Q}$ system is US and so is the energy. Since the US gluons interact with the $Q\bar{Q}$ system, their dynamics is sensitive to the energies of the (non-static) system and hence it is not correct to include them in the static potential. When calculating a physical observable the μ dependence must cancel against μ -dependent contributions coming from the US gluons. Finally it is worth mentioning that the static potential suffers from IR renormalons ambiguities with the following structure

$$\delta V_s \sim C + C_2 r^2 + \dots$$

The constant C is known to be cancelled by the IR pole mass renormalon [47]. The static singlet potential is currently known at NNNLL [70], the only unknown at four loops is the constant term.

The static energy in the perturbative regime has the form

$$E_0(r) = V_s^0(r; \mu) + \delta_{\text{US}}(r, V_s^0, V_o^0, \dots; \mu), \quad (22)$$

where $\delta_{\text{US}}(r, V_s, V_o, V_A, V_B, \dots; \mu)$ (δ_{US} for short) contains contributions from the ultrasoft gluons. As mentioned, $V_s(r; \mu)$ and $V_o(r; \mu)$ do not depend on μ up to N²LO [60]. The former coincides with $E_0(r)$ at this order and the latter may be found in [77]. The fact that the μ dependence of δ_{US} must cancel the one in $V_s(r; \mu)$ is the key observation that leads to a drastic simplification in the calculation of the $\log \alpha_s$ terms

in $E_0(r)$. So, for instance, the logarithmic contribution at $N^3\text{LO}$, which is part of the three-loop contributions to $V_s(r; \mu)$, may be extracted from a one-loop calculation of δ_{US} [59, 60] and the single logarithmic contribution at $N^4\text{LO}$, which is part of the four-loop contributions to $V_s(r; \mu)$, may be extracted from a two-loop calculation of δ_{US} . Notice that we denote $N^n\text{LO}$, contributions to the potential of order α_s^{n+1} and $N^n\text{LL}$, contributions of order $\alpha_s^{n+2} \log^{n-1} \alpha_s$.

The general form of the relativistic corrections to the singlet potential in the center of mass is (we drop the index s for simplicity):

$$V(r) = V^{(0)}(r) + \frac{V^{(1)}(r)}{m} + \frac{V^{(2)}(r)}{m^2} + \dots, \quad (23)$$

$$V^{(2)} = V_{SD}^{(2)} + V_{SI}^{(2)},$$

$$V_{SI}^{(2)} = \frac{1}{2} \left\{ \mathbf{p}^2, V_{\mathbf{p}^2}^{(2)}(r) \right\} + \frac{V_{\mathbf{L}^2}^{(2)}(r)}{r^2} \mathbf{L}^2 + V_r^{(2)}(r), \quad (24)$$

$$V_{SD}^{(2)} = V_{LS}^{(2)}(r) \mathbf{L} \cdot \mathbf{S} + V_{S^2}^{(2)}(r) \mathbf{S}^2 + V_{S_{12}}^{(2)}(r) \mathbf{S}_{12}(\hat{\mathbf{r}}),$$

$\mathbf{S} = \mathbf{S}_1 + \mathbf{S}_2$, $\mathbf{L} = \mathbf{r} \times \mathbf{p}$, $\mathbf{S}_1 = \boldsymbol{\sigma}_1/2$, $\mathbf{S}_2 = \boldsymbol{\sigma}_2/2$, and $\mathbf{S}_{12}(\hat{\mathbf{r}}) \equiv 3\hat{\mathbf{r}} \cdot \boldsymbol{\sigma}_1 \hat{\mathbf{r}} \cdot \boldsymbol{\sigma}_2 - \boldsymbol{\sigma}_1 \cdot \boldsymbol{\sigma}_2$.

We see that differently from what discussed previously the corrections to the potential start at order $1/m$. The potential proportional to $V_{LS}^{(2)}$ may be identified with the spin-orbit potential, the potential proportional to $V_{S^2}^{(2)}$ with the spin-spin potential and the potential proportional to $V_{S_{12}}^{(2)}$ with the spin tensor potential. The above potentials read at leading (non-vanishing) order in perturbation theory (see, e.g., Ref. [47]):

$$V^{(1)}(r) = -\frac{2\alpha_s^2}{r^2}, \quad (25)$$

$$V_r^{(2)}(r) = \frac{4\pi}{3} \alpha_s \delta^{(3)}(\mathbf{r}), \quad V_{p^2}^{(2)}(r) = -\frac{4\alpha_s}{3r}, \quad V_{L^2}^{(2)}(r) = \frac{2\alpha_s}{3r}, \quad (26)$$

$$V_{LS}^{(2)}(r) = \frac{2\alpha_s}{r^3}, \quad V_{S^2}^{(2)}(r) = \frac{16\pi\alpha_s}{9} \delta^{(3)}(\mathbf{r}), \quad V_{S_{12}}^{(2)}(r) = \frac{\alpha_s}{3r^3}. \quad (27)$$

These potentials and the static octet potential have been calculated at higher order in perturbation theory see e.g. [47, 76, 77]. Once one has obtained the potentials as matching coefficients of pNRQCD one can start doing calculations inside the EFT obtaining for example the energy levels of quarkonium [78, 79]. Nonperturbative effects in the form of local or time nonlocal chromoelectric correlators start to appear at order α_s^5 i.e. at NNNLO [47, 76]: their contribution is suppressed.

The case of baryons made by three heavy quarks or two heavy quarks and a light quark has also been addressed in pNRQCD [96] and the static three quark potential has been calculated at one loop accuracy, showing some interesting features [97].

Strongly coupled pNRQCD

When $mv \sim \Lambda_{\text{QCD}}$, we speak about strongly-coupled pNRQCD because the soft scale is nonperturbative and the matching from NRQCD to pNRQCD is nonperturbative i.e. it cannot be performed within an expansion in α_s . In this case, since we work at a nonperturbative scale, only color singlet degrees of freedom remain dynamical and they include $Q\bar{Q}$ states, hybrids $Q\bar{Q}g$ states and glueballs (and if we consider light quarks as part of the binding, color singlet states formed by a heavy quark and heavy antiquark and light quarks, as in the case of tetraquarks). Since the physics is nonperturbative we need to use input coming from the lattice to construct the EFT. In particular we can use the lattice evaluation of the gluonic static energies of a $Q\bar{Q}$ pair: they have been calculated since long [80, 81] and recently updated [85]. Such lattice calculations use insertions of gluonic fields at the initial and final Schwinger strings, inside a generalized static Wilson loop, to select some given symmetries. The gluonic static energies, E_F in Fig. 8, are classified according to representations of the symmetry group $D_{\infty h}$, typical of diatomic molecules, and labeled by Λ_η^σ (see Fig. 7): Λ is the rotational quantum number $|\hat{\mathbf{r}} \cdot \mathbf{K}| = 0, 1, 2, \dots$, with \mathbf{K} the angular momentum of the gluons, that corresponds to $\Lambda = \Sigma, \Pi, \Delta, \dots$; η is the CP eigenvalue ($+1 \equiv g$ (gerade) and $-1 \equiv u$ (ungerade)); σ is the eigenvalue of reflection with respect to a plane passing through the $Q\bar{Q}$ axis. The quantum number σ is relevant only for Σ states. In general there can be more than one state for each irreducible representation of $D_{\infty h}$: higher states are denoted by primes, e.g., $\Pi_u, \Pi'_u, \Pi''_u, \dots$. Notice that this set of static energies will be fundamental later to address the exotics.

Since at this moment we are dealing with $Q\bar{Q}$ states below threshold we are interested merely in the Σ_g^+ static energy (that in this case coincides with the static singlet $Q\bar{Q}$ potential) and in the information that such curve develops a gap of order Λ_{QCD} at a distance $r \sim \Lambda_{\text{QCD}}^{-1}$: therefore all the hybrid static energies can be integrated out as pNRQCD follows from integrating out all degrees of freedom with energy up to mv^2 . The quarkonium singlet field S is now the only low-energy dynamical degree of freedom in the pNRQCD Lagrangian (up to US pions) which reads [62, 63, 47]:

$$L_{\text{pNRQCD}} = \int d^3R \int d^3r S^\dagger \left(i\partial_0 - \frac{\mathbf{p}^2}{2m} - V_S(r) \right) S \quad (28)$$

and lends support to potentials models in this particular regime. Indeed Eq. (28) originates a Schrödinger equation governed by the singlet potential.

The nonperturbative QCD potential

The difference with the phenomenological potential models is that now the singlet potential $V_s(r) = V_0 + V^{(1)}/m + V^{(2)}/m^2$, is the QCD potential calculated in the matching obtained in [62, 63] and display novel characteristics. These potentials are nonperturbative and are given in terms of generalized Wilson loops. However relevant differences emerge also with respect to the Wilson loop approach. The general decomposition of the potential is of the form of Eq. (23). It features a contribution already at order $1/m$ [62] given in terms of a novel expectation value of a static Wilson

loop with insertion of a chromoelectric field. The potential at order $1/m^2$ appears factorized in the product of NRQCD matching coefficients, carrying contribution in the $\log(m/\mu)$ and generalized Wilson loops with chromomagnetic and chromoelectric insertions. This solves the problem of the incompatibility of the Wilson loop potentials and the perturbative calculation. Moreover, additional generalized Wilson loops contribution of novel type emerge see [63, 47] for all the explicit expressions. Spin effects in quarkonium are appearing only at order $1/m^2$ and are therefore suppressed in the spectrum and in the transitions: we will see that things are different for exotics. Some of these generalized Wilson loops have been calculated on the lattice (only quenched) [82, 42, 83, 84] but some contributions at order $1/m^2$ are still to be calculated. The EFT then lends a clean definition and an interpretation of the static Wilson loops measured on the lattice as actual potentials in this regime, together with a prescription to use them to calculate observables. Once the nonperturbative potentials are given in terms of generalized Wilson loops one can use a model of low energy QCD to evaluate them. A minimal area law for example gives for the potentials of Eq.(??) a linear term for $V^{(0)}(r) = \sigma r$ and $V_{L^2}^{(2)}(r) = -\frac{\sigma}{6}r$ and nonzero contributions to $V_r^{(2)}(r)$ and $V_{LS}^{(2)}(r)$. The velocity dependent relativistic nonperturbative contribution corresponds to the angular momentum and the energy of the flux tube between the quark and the antiquark while the one in the spin dependent part is relevant to obtain agreement with the fine separations of the quarkonia multiplets (as it was pursued previously using a scalar confinement kernel in the Bethe-Salpeter equation). These findings are in agreement with what is obtained from the lattice calculations of the Wilson loops. Using a QCD effective string model add several further subleading corrections see [110, 111].

Using these potentials, all the masses for heavy quarkonia below threshold can be obtained by solving the Schrödinger equation with such potentials. Lorentz invariance is still there in the form of exact relations among potentials and it has been observed on the lattice. Decays are described by calculating the imaginary parts of the potentials [93] where nonperturbative contributions enter in the form of gauge invariant time non local chromoelectric and chromomagnetic correlators that have still to be calculated on the lattice. Summarizing, strongly coupled pNRQCD factorizes low energy nonperturbative contributions in terms of generalised gauge invariant Wilson loops, opening the way to a systematic study of the confinement mechanism and systematic applications to quarkonium spectrum and decay as we will see in the dedicated section.

The three heavy quark static potential has been studied on the lattice using Wilson loops [98, 99].

Spectra, transitions, decays and production, SM parameters extractions

Together with lattice, pNRQCD is the theoretical framework that is nowadays mostly used for calculations and predictions of quarkonium properties. The power counting of the EFT allows to attach an error to each prediction. In the regime in which the soft scale is perturbative, pNRQCD enables precise and systematic higher order calculations on bound state allowing the extraction of precise determinations of standard model parameters like the quark masses and α_s . For example, based on Eq. (22), it has been possible to use lattice calculations of the static energy with 2+1 flavour and the NNNLO pNRQCD calculation of the static energy, including the US log resummation, to extract a precise determination of α_s at rather low energy and run it at the mass of the Z, obtaining $\alpha_s(M_Z) = 0.11660^{+0.00110}_{-0.00056}$, which is a competitive extraction made at a pretty high orders of the perturbative expansion [86, 70, 71]. This method of α_s extraction is now used by several groups, see e.g. [72, 75] and the force, defined in terms of a single chromoelectric insertion in the Wilson loop could be used as well [117, 118].

In the same way one can extract precise determinations of the bottom and charm masses using the experimental measurements of the mass of the lowest states and comparing it to the formula for the energies in pNRQCD at NNNLO, which depends on the mass in a given scheme. The renormalon ambiguity cancels between the mass and the static potential and a pretty good determination is possible see e.g. [73, 74] and references therein. Moreover, the energy levels of some of the lowest quarkonia states have been obtained at high orders in perturbation theory using weakly coupled pNRQCD showing that the constant separation on the energy levels may be generated in this way, see e.g. [87, 87, 94, 95] Electromagnetic M1 and E1 transitions have been calculated in pNRQCD, see e.g. [88, 89, 90, 91]. There are so many results that it is impossible to discuss all of them here and we refer you to some reviews [76, 47, 26, 28, 27].

For what concern production it is very promising that by factorizing the quarkonium productions cross section at lower energy in pNRQCD [119, 120, 121], one can rewrite the octet NRQCD LDMEs, which are the nonperturbative unknowns, in terms of product of wave functions and gauge invariant low energy correlators that depend only on the glue and not the on flavor quantum numbers. This allows us to reduce by half the number of nonperturbative unknowns and promises to have a great impact in the progress of the field.

Confinement and low energy QCD models

Strongly coupled pNRQCD realizes a scale factorization encoding the low energy physics in generalized gauge invariant Wilson loops, i.e. Wilson loops with insertions of chromoelectric and chromomagnetic fields. Such objects no longer depends

on the heavy quark degrees of freedom and on the quark flavor. It turns out that this is a systematic method to study the QCD confinement properties and put them directly in relation to the quarkonium phenomenology. Indeed lattice QCD seems more suitable to ask 'what' instead of 'why' and to understand the mechanism underlying confinement it may be useful to build models of low energy QCD and compare to the lattice results: the interface is offered by the EFT. We have seen that the area law emerging in the static Wilson loop at large distance is responsible of confinement, this in turn corresponds to the formation of a chromoelectric flux tube between the quark and the antiquark that sweeps the area of the Wilson loop, see Fig. 9. This effects is originated by the nonperturbative QCD vacuum that could be imagined as a disordered medium with whirlpools of colour on different scales, thus densely populated by fluctuating fields whose amplitude is so large that they cannot be described by perturbation theory. A QCD vacuum model can be established by making an assumption on the behaviour of the Wilson loop that gives the static potential. The relativistic corrections that involve insertions of gluonic fields in the Wilson loop follow then via functional derivative with respect to the quark path see [52, 13]. Then, one can notice for example that the part proportional to the square of the angular momentum in the of the V_{vd} potential obtained in strongly coupled pNRQCD takes into account the energy and the angular momentum of the flux tube, which is something that could not be obtained in any Bethe Salpeter approach with a confinement scalar convolution kernel. Lattice simulations of the action density or the energy density between the static quark and the static antiquark show indeed a chromoelectrix flux tube configuration see Fig. 9 from ref. [100] and more recent calculations in [101, 102, 103]. The mechanism underlying confinement and flux tube formation has been investigated since long on the lattice [104] using the Wilson loops and the 't Hooft abelian projection, to identify the roles of magnetic monopoles [114, 115] and center vortices, see e.g. the review [27].

In the continuum several models of low energy QCD has been used to explain the flux tube formation ranging from the dual Meissner effect and a dual abelian Higgs model picture, dual QCD [105], the stochastic vacuum [107], the flux tube model [106] and an effective QCD string description. Each of these models can be used to obtain analytic estimates of the behaviour of the generalized Wilson loops for large distance, which in turn give the static potential and the relativistic corrections V_1, V_{sd}, V_{vd} as function of r , see [108, 112, 109, 110, 111]. Similar nonperturbative configurations leading to confinement can be studied analyzing the Wilson loop in case of baryons with three or two heavy quarks [113, 116].

BOEFT and XYZ exotics

Exotic states, i.e. states with a composition different from a quark-antiquark or three quarks in a color singlet, have been predicted before and after the advent of QCD. In the last decades a large number of states, either with a manifest different composition (with isospin and electric charge different from zero) or with other exotic char-

acteristics have been observed in the sector with two heavy quarks $Q\bar{Q}$, at or above the quarkonium strong decay threshold at the B-Factories, tau-charm and LHC and Tevatron collider experiments [123, 26, 28, 122]. These states have been termed X, Y, Z in the discovery publications, without any special criterion, apart from Y being used for exotics with vector quantum numbers, i.e., $J^{PC} = 1^{--}$. Meanwhile, the Particle Data Group (PDG) has proposed a new naming scheme [124], that extends the scheme used for ordinary quarkonia, in which the new names carry information on the J^{PC} quantum numbers, see [123] for more details. Some of these exotics have quantum numbers that cannot be obtained with ordinary hadrons. In this case, the identification of these states as exotic is straightforward. In the other cases, the distinction requires a careful analysis of experimental observations and theoretical predictions. Of course all hadrons should be color singlets but allowing combinations beyond the $Q\bar{Q}$ and QQQ in the two heavy quarks sector calls for tetraquarks like $Q\bar{Q}q\bar{q}$, $QQ\bar{q}\bar{q}$, pentaquarks like $Q\bar{Q}qqq$, hybrids $Q\bar{Q}g$ and so on [126]. We have observed these exotics up to now only in the sector with two heavy quarks likely due to the fact that the presence of the two heavy quarks stabilizes them. Some of the discovered states have an unprecedentedly small width even if they are at or above the strong decay threshold. XYZ states offer us unique possibilities for the investigation of the dynamical properties of strongly correlated systems in QCD: we should develop the tools to gain a solid interpretation from the underlying field theory, QCD. This is a very significant problem with trade off to other fields featuring strong correlations and a pretty interesting connections to heavy ion physics, as propagation of these states in medium may help us to scrutinize their properties.

Since the new quarkonium revolution i.e. the discovery of the first exotic state, the $X(3872)$ at BELLE in 2003 [125], a wealth of theoretical papers appeared to supply interpretation and understanding of the characteristics of the exotics. Many models are based on the choice of some dominant degrees of freedom and an assumption on the related interaction hamiltonian. An effective field theory molecular description of some of these states particularly close to threshold was also put forward, see e.g. [128, 127, 129, 130, 131]. A priori the simplest system consisting of only two quarks and two antiquarks (generically called tetraquarks) is already a very complicated object and it is unclear whether or not any kind of clustering occurs in it. However, to simplify the problem it is common to focus on certain substructures and investigate their implications: in hadroquarkonia the heavy quark and antiquark form a compact core surrounded by a light-quark cloud; in compact tetraquarks the relevant degrees of freedom are compact diquarks and antidiquarks; in the molecular picture two color singlet mesons are interacting at some typical distance, for a review see [123]. Discussions about exotics therefore often concentrate on the 'pictures' of the states, like for example the tetraquark interpretation against the molecular one (of which both several different realizations exist). However, as a matter of fact all the light degrees of freedom (light quarks, glue, in different configurations) should be there in QCD close or above the strong decay threshold: it is a result of the strong dynamics which one sets in and which configuration dominates in a given regime.

Even in an ordinary quarkonium or in a heavy baryon, which has a dominant $Q\bar{Q}$ or QQQ configuration, subleading contributions of the quantum field theoretical Fock space may contribute, with have additional quark-antiquark pairs and active gluons. However, in the most interesting region, close or above the strong decay threshold, where the X Y Z have been discovered, the situation is much more complicated: there is no mass gap between quarkonium and the creation of a heavy-light mesons couple, nor to gluon excitations, therefore many additional states built on the light quark quantum numbers may appear [122]. Still, m is a large scale and a first scale factorization is applicable so that Nonrelativistic QCD is still valid. Then, if we want to introduce a description of the bound state similar to pNRQCD, making apparent that the zero order problem is the Schrödinger equation, we can still count on another scale separation. Let us consider bound states of two nonrelativistic particles and some light d.o.f., e.g. molecules in QED or quarkonium hybrids ($Q\bar{Q}g$ states) or tetraquarks ($Q\bar{Q}q\bar{q}$ states) in QCD: electron/gluon fields/light quarks change adiabatically in the presence of heavy quarks/nuclei. The heavy quarks/nuclei interaction may be described at leading order in the nonrelativistic expansion by an effective static energy (or potential) E_κ between the static sources where κ labels different excitations of the light degrees of freedom. A plethora of states can be built on each on the static energies E_κ by solving the corresponding Schrödinger equation. This picture corresponds to the Born-Oppenheimer (BO) approximation [80, 132, 133]. Starting from pNRQED/pNRQCD the BO approximation can be made rigorous and cast into a suitable EFT called Born-Oppenheimer EFT (BOEFT) [136, 137, 141, 140, 138, 139, 123] which exploits the hierarchy of scales $\Lambda_{\text{QCD}} \gg mv^2$, v being the velocity of the heavy quark.

In [136] we have obtained the BOEFT that describes hybrids. In particular we have obtained the static potentials and the set of coupled Schrödinger equations, solved them and produced all the hybrids multiplets, see Fig. 12, for the case of the two first static energies Σ_u^- and Π_u . Such static energies are degenerated at short distance where the cylindrical symmetry gets subdue to a $O(3)$ symmetry and are then labelled by the quantum number of a gluonic operator 1^{+-} called a gluelump. The hybrid static energies are described by a repulsive octet potential plus the gluelump mass in the short distance limit and the $O(3)$ symmetry is broken at order r^2 of the multipole expansion. In the long distance regime the static energies display a linear r behaviour. The gluelump correlator can be calculated on the lattice to determine the gluelump mass. It is depending on the scheme used (the scheme dependence cancels against the analogous dependence in the quark mass and in the octet static potential) but it is of the order of 800 MeV. The hybrid multiplets H_i are constructed from the solution of the Schrödinger equations in correspondence of their J^{PC} quantum numbers. The coupling between the different Schrödinger equations is induced by a nonadiabatic coupling, known in the Born Oppenheimer description of diatomic molecules, induced by the noncommutation between the kinetic term and a projector of the cylindrical symmetry in the BOEFT lagrangian.

The degeneracy of the static energies at small distance induces a phenomenon called Λ doubling, removing the degenerations between multiplets of opposite parity. This phenomenon is known in molecular physics but with smaller size. This and

the structure of the multiplets differ from what is obtained in models for the hybrids, cf. [136]. We used lattice input on the hybrid static energies and on the gluelump mass.

In [138, 139] we obtained the spin dependent potentials at order $1/m$ and $1/m^2$ in the quark mass expansion and we could calculate all the hybrids spin multiplets. Notice that on one hand it is seldom to find the spin interaction considered in models, on the other hand it would be different. In fact the $1/m$ contributions couple the angular momentum of the gluonic excitation with the total spin of the heavy-quark-antiquark pair. These operators are characteristic of the hybrid states and are absent for standard quarkonia. Among the $1/m^2$ operators besides the standard spin-orbit, total spin squared, and tensor spin operators respectively, which appear for standard quarkonia, three novel operators appear. So interestingly, differently from the quarkonium case, the hybrid potential gets a first contribution already at order Λ_{QCD}^2/m . Hence, spin splittings are remarkably less suppressed in heavy quarkonium hybrids than in heavy quarkonia: this will have a notable impact on the phenomenology of exotics. We extracted the nonperturbative low energy correlators appearing in the factorization fixing them on lattice data on the masses of charmonium hybrids and we could then predict all the bottomonium hybrids spin multiplets, that are more difficult to evaluate on the lattice. In this same framework it is also possible to calculate hybrids decays and quarkonium/hybrids mixing [141, ?]. The BOEFT may be used to describe also tetraquarks, double heavy baryons and pentaquarks [137, 140]. In the case of tetraquarks, a necessary input of the theory is the calculation of the lattice generalized Wilson loops with appropriate symmetry and light quark operators, so that besides the quantum number κ also the isospin quantum numbers $I = 0, 1$ have to be considered. The BOEFT approach reconciles the different pictures of exotics based on tetraquarks, molecules, hadroquarkonium . . . In fact in the plot of a static energy as a function of r for a state with $Q\bar{Q}q\bar{q}$ or $Q\bar{Q}g$ we will have different regions: for short distance a hadroquarkonium picture would emerge, then a tetraquark (or hybrid) one and when passing the heavy-light mesons line, avoided cross level effects should have to be taken into account and a molecular picture would emerge. However QCD would dictate, through the lattice correlators and the BOEFT characteristics and power counting, which structure would dominate and in which precise way. In addition production and suppression in medium may be described in the same approach [119, 168]. Production of hybrid states have been studied in [134, 135].

pNRQCD at finite T , open quantum system and quarkonium in medium

Quarkonium is a special probe also for deconfinement, besides confinement. A prediction of QCD is that at a certain value of temperature (or energy density) hadronic matter undergoes a transition to a deconfined state of quarks and gluons called the quark-gluon plasma (QGP). Lattice QCD have shown that such transition takes

place at a critical temperature around 150 MeV [43, 142]. Experimentally heavy ion collisions make it possible to study strongly interacting matter under extreme conditions in the laboratory, recreating the QGP that should have primordially existed microseconds after the Big Bang. These experiments have therefore a great importance also for cosmology and allows to investigate the nuclear matter phase diagram, i.e. how nuclear matter change by varying the temperature and the chemical potential, see [27, 29]. In heavy ions experiments at the LHC at CERN and at the RHIC at BNL the produced matter is characterized by small net baryon densities and high temperature. [43]. Heavy quarks are good probes of the QGP. They are produced at the beginning of the collision and remain up to the end. The heavy quark mass m introduces a large scale, whose contribution may be factorized and computed in perturbation theory. Low-energy scales are sensitive to the temperature T and even if nonperturbative they may be accessible via lattice calculations (for what concerns equilibrium physics). As we discussed, quarkonia are special hard probes as they are multi-scale systems. In the hot QCD medium also the thermal scales of the Quark Gluon Plasma (QGP) are emerging: the scale related to the temperature $(\pi)T$, the Debye mass $m_D \sim gT$ related to the (chromo) electric screening and the scale g^2T related to the (chromo)magnetic screening. In a weakly coupled plasma the scales are separated and hierarchically ordered, in a strongly coupled plasma $m_D \sim T$. To address QCD at finite T calculations, EFTs have been developed too to resum contributions related to the thermal scales and to address IR sensitivities. In real time the Hard Thermal Loop EFT (HTL) [144, 145] is taking care of integrating out the temperature scale.

Heavy quarkonium dissociation has been proposed long time ago as a clear probe of the quark-gluon plasma formation in colliders through the measurement of the dilepton decay-rate signal- In [143] this was related to the screening of the quark-antiquark interaction due to Debye mass and it was suggested that this would have manifested in an exponential screening term $\exp(-m_D r)$ in the static potential. One of the key quantities measured in experiments is the nuclear modification factor $R_{AA} = Y(PbPb)/(N_{coll}Y(pp))$ where $Y(PbPb)$ and $Y(pp)$ are the quarkonium yield in PbPb and in pp collisions respectively. R_{AA} is a measure for the difference in particle production in pp and nucleus-nucleus collisions. Since higher excited quarkonium states have larger radius then the expectation was that, as the temperature increases, quarkonium would dissociate subsequently from the higher to the lower states giving origin to sequential melting. In order to study quarkonium properties in a thermal bath at a temperature T , the quantity to be determined is the quarkonium potential V which dictates, through the Schrödinger equation the real-time evolution of the wave function of a $Q\bar{Q}$ pair in the medium. This has been investigated for years using many phenomenological assumptions, spanning from the internal energy to the free energy, either the average free energy or the singlet one which is gauge dependent. pNRQCD has given us the possibility to define in QCD what is this potential: it is the matching coefficient of the EFT that results from the integration of all the scales above the scale of the binding energy. In a series of papers [148, 149, 151, 150, 152, 147] a pNRQCD at finite T description has been constructed. One has to proceed integrating out all scales up to the binding energy and

if the temperature is higher than the binding energy then also the temperature has to be integrated out using HTL EFT. When T is bigger than the energy, the potential depends on the temperature, otherwise not. Thermal effects appear in any case in the nonpotential contributions to the energy levels. We assumed that the bound state exist for $T \ll m$ and $1/r \geq m_D$, we worked in the weak coupling limit and we consider all possible scales hierarchies [148]. We found that the thermal part of the potential has a real part (roughly described by the free energy) and an imaginary part. The imaginary part comes from two effects: the Landau damping [146, 152, 148], an effect existing also in QED, and the singlet to octet transition, existing only in QCD [148]. Which one dominates depends on the ratio between m_D and E . In the EFT one could show that the imaginary part of the potential related to the Landau damping comes from inelastic parton scattering [151] and the singlet to octet transition from gluon dissociation [150]. The existence of the imaginary part, first realized in [146] changed our paradigm for quarkonium suppression as the state dissociates for this reason well before that the conventional screening becomes active [146, 152]. The pattern of thermal corrections is pretty interesting [148]: when $T < E$ thermal corrections are only in the energy; for $T > 1/r, 1/r > m_D$ or $1/r > T > E$ there is no exponential screening and T dependent power like corrections appear; if $T > 1/r, 1/r \sim m_D$ we have exponential screening but the imaginary part of the static potential is already bigger than the real one and dissociation already happened. Once the potential has been calculated, the EFT gives the systematic framework to obtain the thermal energies: in [149] it was performed the first QCD calculation of the thermal contributions to the $\Upsilon(1S)$ mass and width at order $m\alpha_s^5$ at LHC below the dissociation temperature of about 500 MeV. This calculation is very important because it gives the parametric T dependence of this observables. The width goes linear in T in the dominant term and this has been confirmed by lattice calculations of the spectrum [153]. These findings in the EFT in perturbation theory have inspired many subsequent nonperturbative calculations of the static potential at finite T . In particular the Wilson loop at finite T has been calculated on the lattice [154, 155] finding hints of a large imaginary parts. These calculations are pretty challenging and refining of the extraction methods are currently in elaboration [156].

Free energies defined by Polyakov loop correlators have been always very prominent in QCD at finite T , see e.g. the reviews [163, 157]. The Polyakov loop correlators of a single heavy quark and of a quark-antiquark pair have been calculated both in perturbation theory using pNRQCD to resum scales contributions in [159, ?, 158, 160] and on the lattice to obtain these quantities fully nonperturbatively in [162, 161]. In particular: the Polyakov loop has been computed up to order g^6 , the (subtracted) $Q\bar{Q}$ free energy has been computed at short distances up to corrections of order $g^7(rT)^4$, g^8 , the (subtracted) $Q\bar{Q}$ free energy has been computed at screening distances up to corrections of order g^8 ; the singlet free energy has been computed at short distances up to corrections of order $g^4(rT)^5$, g^6 ; the singlet free energy has been computed at screening distances up to corrections of order g^5 [159, 158, 160]. From the lattice simulations and from comparison to the perturbative results some interesting information can be obtained [162, 161]: lattice calculations are consistent with weak-coupling expectations in the regime of application of the weakly coupled

resummed perturbation theory which confirms the predictive power of the EFT; the crossover temperature to the quark-gluon plasma is $153 + 6.5 - 5$ MeV as extracted from the entropy of the Polyakov loop; the screening sets in at $rT \sim 0.3 - 0.4$ (observable dependent), consistent with a screening length of about $1/m_D$; asymptotic screening masses are about $2m_D$ (observable dependent); the first determination of the color octet $Q\bar{Q}$ free energy has been obtained [161]. The free energies turn out not to be the objects to be used as a potential in the Schrödinger equation even if the singlet free energy may provide a good approximation of the real part of the static potential.

These are all results in thermal equilibrium. However, the evolution of quarkonium in the QGP is an out of equilibrium process in which many effects enter: the hydrodynamical evolution of the plasma and the production, dissociation and regeneration of quarkonium in the medium, to quote the most prominent ones. It is necessary therefore to introduce an appropriate framework to describe the real time nonequilibrium evolution of quarkonium in the QGP medium. This has been realized in [165, 164, 166] where an open quantum system (OQS) framework rooted in pNRQCD at finite T has been developed that is fully quantum, conserves the number of heavy quarks and considers both color singlet and color octet quarkonium degrees of freedom. For a review of open quantum system approach see [171, 172, 176, 175] and references therein.

We consider the density matrix associated to our system. We distinguish between the environment (QGP), characterized by the scale T , and the subsystem of system (quarkonium) characterized by the scale E . We identify the inverse of E with the intrinsic time scale of the subsystem: $\tau_S \sim 1/E$ and the inverse of πT with the correlation time of the environment: $\tau_E \sim 1/(\pi T)$. If the medium is in thermal equilibrium, or locally in thermal equilibrium, we may understand T as a temperature, otherwise is just a parameter. The medium can be strongly coupled. Then we trace the density matrix over the environment and we are left with a color singlet and color octet density matrix that can be written in terms of the pNRQCD fields, working in the close time path formalism. The evolution of the system is characterized by a relaxation time τ_R that is estimated by the inverse of the color singlet self-energy diagram in pNRQCD at finite T . We select quarkonia states with a small radius (Coulombic) for which $1/r \gg \pi T, \Lambda_{QCD}$ and we consider $\pi T \gg E$. In this framework, in [164], a set of master equations governing the time evolution of heavy quarkonium in a medium can be derived. The equations follow from assuming the inverse Bohr radius of the quarkonium to be greater than the energy scale of the medium, and model the quarkonium as evolving in the vacuum up to a time $t = t_0$ at which point interactions with the medium begin. The equations express the time evolution of the density matrices of the heavy quark-antiquark color singlet, ρ_s , and octet states, ρ_o , in terms of the color singlet and octet Hamiltonians, $h_s = \mathbf{p}^2/M - C_F \alpha_s/r + \dots$ and $h_o = \mathbf{p}^2/M + \alpha_s/(2N_c r) + \dots$, and interaction terms with the medium, which, at order r^2 in the multipole expansion, are encoded in the self-energy diagrams of the EFTs. These interactions account for the mass shift of the heavy $Q\bar{Q}$ pair induced by the medium, its decay width induced by the medium, the generation of $Q\bar{Q}$ color singlet states from $Q\bar{Q}$ color octet states interacting with the medium and the gener-

ation of $Q\bar{Q}$ color octet states from $Q\bar{Q}$ (color singlet or octet) states interacting with the medium (recombination terms). Both Landau damping and singlet to octet effects are contained in the self energy. The leading order interaction between a heavy $Q\bar{Q}$ field and the medium is encoded in pNRQCD in a chromoelectric dipole interaction, which appears at order r/m^0 in the EFT Lagrangian. The approach gives us master equations, in general non Markovian, for the out of equilibrium evolution of the color singlet and color octet matrix densities. The system is in non-equilibrium because through interaction with the environment (quark gluon plasma) singlet and octet quark-antiquark states continuously transform in each other although the total number of heavy quarks is conserved.

Assuming that any energy scale in the medium is larger than the heavy $Q\bar{Q}$ binding energy E , in particular that $\tau_R \gg \tau_E$, we obtain a Markovian evolution while the chosen hierarchy of scales implies $\tau_s \gg \tau_E$ qualifying the regime as quantum Brownian motion. In this situation we can reduce the general master equation to a Linblad form. In this case the properties of the QGP are encoded in two transport coefficients: the heavy quark momentum diffusion coefficient, κ , and its dispersive counterpart γ which are given by time integrals of appropriate gauge invariant correlators at finite T given by the integral of gauge invariant finite T QCD correlators of chromoelectric fields:

$$\kappa = \frac{g^2}{6N_c} \int_0^\infty ds \left\langle \{E^{a,i}(s, \mathbf{0}), E^{a,i}(0, \mathbf{0})\} \right\rangle, \quad (29)$$

$$\gamma = -i \frac{g^2}{6N_c} \int_0^\infty ds \left\langle [E^{a,i}(s, \mathbf{0}), E^{a,i}(0, \mathbf{0})] \right\rangle. \quad (30)$$

They come from the pNRQCD self energies that in this regime could be factorized between this contribution and the bound state dependent part. In the case of a nonperturbative QGP, these objects are nonperturbative and should be evaluated on the lattice at a given temperature in an extended window of temperatures [177]. In this way one could use lattice to give input to a nonequilibrium calculation. In a series of papers [167, 168] we have solved the Linblad equation using the highly efficient quantum trajectory method and realistically implementing a 3+1D dissipative hydrodynamics code [169], and we have obtained the bottomonium ($\Upsilon(1S), \Upsilon(2S), \Upsilon(3S)$) nuclear modification factors and the anisotropic flows, see Fig. 13 for a comparison between LHC data and our results on R_{AA} . The computation does not rely on any free parameter, as it depends only on the two transport coefficients that have been evaluated independently in lattice QCD. Our final results, which include late-time feed down of excited states, agree well with the available data from LHC 5.02 TeV PbPb collisions. Notice that the bands in the Fig. 13 depend on the undetermination with which the nonperturbative transport coefficients κ and γ , that are properties of the QGP, are presently known. More precise experimental data can help to narrow down their range. In this way we can use quarkonia with small radii as a diagnostic and investigation tool of the characteristics of the strongly coupled QGP. To apply the same description to charmonium would require to modify the master equations considering terms beyond leading order in the quarkonium

density. Further work in a similar approach at the level of the Boltzmann equation has been done in [173, 174].

Outlook

The great progress of the last few decades in the construction of nonrelativistic effective quantum field theories and the progress in lattice QCD calculation allows to treat heavy quark bound states systematically in QCD. In this way quarkonium becomes a golden probe of strong interactions at zero and finite temperature.

Moreover, quarkonium is the prototype of a nonrelativistic multiscale system. Systems of such kind are ubiquitous in matter and in fields of physics, from particle to nuclear physics, to condensed matter and to astro and cosmological applications and play a key role in several open challenges at the frontier of particle physics. Therefore, all the progress obtained in this framework holds the promise to have an impact in a number of relevant contemporary problems.

For example, combining the techniques of nonrelativistic effective field theories and the open quantum framework, we can address the nonequilibrium evolution of heavy dark matter pairs in the early universe. On the other hand the XYZ exotics bear similarities to atomic and molecular physics, and results obtained in BOEFT can be used in those fields [137, 181] as well as maybe extended to the consideration of strongly correlated system in condensed matter at finite temperature.

In summary, the physics of heavy quarks not only has been and is extremely important for our advancement in nuclear and particle physics, but has the promise to impact also many other nearby fields.

References

1. J. J. Aubert *et al.* [E598], Phys. Rev. Lett. **33**, 1404-1406 (1974) doi:10.1103/PhysRevLett.33.1404
2. J. E. Augustin *et al.* [SLAC-SP-017], Phys. Rev. Lett. **33**, 1406-1408 (1974) doi:10.1103/PhysRevLett.33.1406
3. H. Fritzsch, M. Gell-Mann and H. Leutwyler, Phys. Lett. B **47**, 365-368 (1973) doi:10.1016/0370-2693(73)90625-4
4. S. L. Glashow, J. Iliopoulos and L. Maiani, Phys. Rev. D **2**, 1285-1292 (1970) doi:10.1103/PhysRevD.2.1285
5. W. Fischler, Nucl. Phys. B **129** (1977), 157-174 doi:10.1016/0550-3213(77)90026-8
6. K. G. Wilson, Phys. Rev. D **10**, 2445-2459 (1974) doi:10.1103/PhysRevD.10.2445
7. L. S. Brown and W. I. Weisberger, Phys. Rev. D **20**, 3239 (1979) doi:10.1103/PhysRevD.20.3239
8. M. Creutz, Phys. Rev. D **15**, 1128 (1977) doi:10.1103/PhysRevD.15.1128
9. M. Creutz, Phys. Rev. D **21**, 2308-2315 (1980) doi:10.1103/PhysRevD.21.2308
10. M. Creutz and K. J. M. Moriarty, Phys. Rev. D **26**, 2166 (1982) doi:10.1103/PhysRevD.26.2166
11. S. N. Gupta, S. F. Radford and W. W. Repko, Phys. Rev. D **26**, 3305 (1982) doi:10.1103/PhysRevD.26.3305

12. T. Appelquist, M. Dine and I. J. Muzinich, Phys. Lett. B **69**, 231-236 (1977) doi:10.1016/0370-2693(77)90651-7
13. N. Brambilla and A. Vairo, [arXiv:hep-ph/9904330 [hep-ph]].
14. W. Lucha, F. F. Schoberl and D. Gromes, Phys. Rept. **200**, 127-240 (1991) doi:10.1
15. N. Brambilla, Nuovo Cim. A **105**, 949-958 (1992) doi:10.1007/BF02730836
16. E. E. Salpeter and H. A. Bethe, Phys. Rev. **84**, 1232-1242 (1951) doi:10.1103/PhysRev.84.1232
17. N. Brambilla, Nuovo Cim. A **105**, 949-958 (1992) doi:10.1007/BF02730836
18. H. J. Schnitzer, Phys. Rev. D **18**, 3482 (1978) doi:10.1103/PhysRevD.18.3482
19. G. Buchalla, T. K. Komatsubara, F. Muheim, L. Silvestrini, M. Artuso, D. M. Asner, P. Ball, E. Baracchini, G. Bell and M. Beneke, *et al.* Eur. Phys. J. C **57**, 309-492 (2008) doi:10.1140/epjc/s10052-008-0716-1 [arXiv:0801.1833 [hep-ph]].
20. M. Neubert, Int. J. Mod. Phys. A **11**, 4173-4240 (1996) doi:10.1142/S0217751X96001966 [arXiv:hep-ph/9604412 [hep-ph]].
21. P. Chang, K. F. Chen and W. S. Hou, Prog. Part. Nucl. Phys. **97**, 261-311 (2017) doi:10.1016/j.pnpnp.2017.07.001 [arXiv:1708.03793 [hep-ph]].
22. T. Gershon and V. V. Gligorov, Rept. Prog. Phys. **80**, no.4, 046201 (2017) doi:10.1088/1361-6633/aa5514 [arXiv:1607.06746 [hep-ex]].
23. E. Kou *et al.* [Belle-II], PTEP **2019**, no.12, 123C01 (2019) [erratum: PTEP **2020**, no.2, 029201 (2020)] doi:10.1093/ptep/ptz106 [arXiv:1808.10567 [hep-ex]].
24. A. J. Bevan *et al.* [BaBar and Belle], Eur. Phys. J. C **74**, 3026 (2014) doi:10.1140/epjc/s10052-014-3026-9 [arXiv:1406.6311 [hep-ex]].
25. E. J. Eichten and C. Quigg, Phys. Rev. D **49**, 5845-5856 (1994) doi:10.1103/PhysRevD.49.5845 [arXiv:hep-ph/9402210 [hep-ph]].
26. N. Brambilla, S. Eidelman, B. K. Heltsley, R. Vogt, G. T. Bodwin, E. Eichten, A. D. Frawley, A. B. Meyer, R. E. Mitchell and V. Papadimitriou, *et al.* Eur. Phys. J. C **71**, 1534 (2011) doi:10.1140/epjc/s10052-010-1534-9 [arXiv:1010.5827 [hep-ph]].
27. N. Brambilla, S. Eidelman, P. Foka, S. Gardner, A. S. Kronfeld, M. G. Alford, R. Alkofer, M. Butenschoen, T. D. Cohen and J. Erdmenger, *et al.* Eur. Phys. J. C **74**, no.10, 2981 (2014) doi:10.1140/epjc/s10052-014-2981-5 [arXiv:1404.3723 [hep-ph]].
28. N. Brambilla *et al.* [Quarkonium Working Group], doi:10.5170/CERN-2005-005 [arXiv:hep-ph/0412158 [hep-ph]].
29. A. Andronic, F. Arleo, R. Arnaldi, A. Beraudo, E. Bruna, D. Caffarri, Z. C. del Valle, J. G. Contreras, T. Dahms and A. Dainese, *et al.* Eur. Phys. J. C **76**, no.3, 107 (2016) doi:10.1140/epjc/s10052-015-3819-5 [arXiv:1506.03981 [nucl-ex]].
30. E. Chapon, D. d'Enterria, B. Ducloue, M. G. Echevarria, P. B. Gossiaux, V. Kartvelishvili, T. Kasemets, J. P. Lansberg, R. McNulty and D. D. Price, *et al.* Prog. Part. Nucl. Phys. **122**, 103906 (2022) doi:10.1016/j.pnpnp.2021.103906 [arXiv:2012.14161 [hep-ph]].
31. G. T. Bodwin, E. Braaten, E. Eichten, S. L. Olsen, T. K. Pedlar and J. Russ, [arXiv:1307.7425 [hep-ph]].
32. H. S. Chung, doi:10.1142/9789811219313_0064
33. C. Z. Yuan and S. L. Olsen, Nature Rev. Phys. **1**, no.8, 480-494 (2019) doi:10.1038/s42254-019-0082-y [arXiv:2001.01164 [hep-ex]].
34. S. Joosten and Z. E. Meziani, PoS **QCDEV2017**, 017 (2018) doi:10.22323/1.308.0017 [arXiv:1802.02616 [hep-ex]].
35. G. Barucca *et al.* [PANDA], Eur. Phys. J. A **57**, no.6, 184 (2021) doi:10.1140/epja/s10050-021-00475-y [arXiv:2101.11877 [hep-ex]].
36. E. Eichten, K. Gottfried, T. Kinoshita, K. D. Lane and T. M. Yan, Phys. Rev. D **17**, 3090 (1978) [erratum: Phys. Rev. D **21**, 313 (1980)] doi:10.1103/PhysRevD.17.3090
37. E. Eichten, K. Gottfried, T. Kinoshita, K. D. Lane and T. M. Yan, Phys. Rev. D **21**, 203 (1980) doi:10.1103/PhysRevD.21.203
38. R. Aaij *et al.* [LHCb], Sci. Bull. **65**, no.23, 1983-1993 (2020) doi:10.1016/j.scib.2020.08.032 [arXiv:2006.16957 [hep-ex]].
39. A. S. Kronfeld, Ann. Rev. Nucl. Part. Sci. **62**, 265-284 (2012) doi:10.1146/annurev-nucl-102711-094942 [arXiv:1203.1204 [hep-lat]].

40. H. J. Rothe, World Sci. Lect. Notes Phys. **43**, 1-381 (1992) doi:10.1142/8229
41. J. B. Kogut, Rev. Mod. Phys. **55**, 775 (1983) doi:10.1103/RevModPhys.55.775
42. G. S. Bali, Phys. Rept. **343**, 1-136 (2001) doi:10.1016/S0370-1573(00)00079-X [arXiv:hep-ph/0001312 [hep-ph]].
43. F. Karsch, Nucl. Phys. A **698**, 199-208 (2002) doi:10.1016/S0375-9474(01)01365-3 [arXiv:hep-ph/0103314 [hep-ph]].
44. M. Campostrini, K. J. M. Moriarty, J. Potvin and C. Rebbi, Phys. Lett. B **193**, 78-84 (1987) doi:10.1016/0370-2693(87)90459-X
45. M. Neubert, doi:10.1142/9789812773579_0004 [arXiv:hep-ph/0512222 [hep-ph]].
46. H. Georgi, HUTP-91-A039.
47. N. Brambilla, A. Pineda, J. Soto and A. Vairo, Rev. Mod. Phys. **77**, 1423 (2005) [arXiv:hep-ph/0410047 [hep-ph]].
48. E. Eichten and F. Feinberg, Phys. Rev. D **23**, 2724 (1981) doi:10.1103/PhysRevD.23.2724
49. D. Gromes, Z. Phys. C **26**, 401 (1984) doi:10.1007/BF01452566
50. A. Barchielli, E. Montaldi and G. M. Prosperi, Nucl. Phys. B **296**, 625 (1988) [erratum: Nucl. Phys. B **303**, 752 (1988)] doi:10.1016/0550-3213(88)90036-3
51. A. Barchielli, N. Brambilla and G. M. Prosperi, Nuovo Cim. A **103**, 59 (1990) doi:10.1007/BF02902620
52. N. Brambilla, P. Consoli and G. M. Prosperi, Phys. Rev. D **50**, 5878-5892 (1994) doi:10.1103/PhysRevD.50.5878 [arXiv:hep-th/9401051 [hep-th]].
53. G. T. Bodwin, E. Braaten and G. P. Lepage, Phys. Rev. D **51**, 1125-1171 (1995) [erratum: Phys. Rev. D **55**, 5853 (1997)] doi:10.1103/PhysRevD.55.5853 [arXiv:hep-ph/9407339 [hep-ph]].
54. W. E. Caswell and G. P. Lepage, Phys. Lett. B **167**, 437-442 (1986) doi:10.1016/0370-2693(86)91297-9
55. G. P. Lepage, L. Magnea, C. Nakhleh, U. Magnea and K. Hornbostel, Phys. Rev. D **46**, 4052-4067 (1992) doi:10.1103/PhysRevD.46.4052 [arXiv:hep-lat/9205007 [hep-lat]].
56. G. C. Nayak, J. W. Qiu and G. F. Sterman, Phys. Rev. D **72**, 114012 (2005) doi:10.1103/PhysRevD.72.114012 [arXiv:hep-ph/0509021 [hep-ph]].
57. G. T. Bodwin, H. S. Chung, J. H. Ee, U. R. Kim and J. Lee, Phys. Rev. D **101**, no.9, 096011 (2020) doi:10.1103/PhysRevD.101.096011 [arXiv:1910.05497 [hep-ph]].
58. A. Pineda and J. Soto, Nucl. Phys. B Proc. Suppl. **64**, 428-432 (1998) doi:10.1016/S0920-5632(97)01102-X [arXiv:hep-ph/9707481 [hep-ph]].
59. N. Brambilla, A. Pineda, J. Soto and A. Vairo, Phys. Rev. D **60**, 091502 (1999) doi:10.1103/PhysRevD.60.091502 [arXiv:hep-ph/9903355 [hep-ph]].
60. N. Brambilla, A. Pineda, J. Soto and A. Vairo, Nucl. Phys. B **566**, 275 (2000) doi:10.1016/S0550-3213(99)00693-8 [arXiv:hep-ph/9907240 [hep-ph]].
61. <https://einrichtungen.ph.tum.de/T30f/tumqcd/index.html>
62. N. Brambilla, A. Pineda, J. Soto and A. Vairo, Phys. Rev. D **63**, 014023 (2001) doi:10.1103/PhysRevD.63.014023 [arXiv:hep-ph/0002250 [hep-ph]].
63. A. Pineda and A. Vairo, Phys. Rev. D **63**, 054007 (2001) [erratum: Phys. Rev. D **64**, 039902 (2001)] doi:10.1103/PhysRevD.64.039902 [arXiv:hep-ph/0009145 [hep-ph]].
64. A. V. Manohar, Phys. Rev. D **56**, 230-237 (1997) doi:10.1103/PhysRevD.56.230 [arXiv:hep-ph/9701294 [hep-ph]].
65. N. Brambilla, D. Gromes and A. Vairo, Phys. Lett. B **576**, 314-327 (2003) doi:10.1016/j.physletb.2003.09.100 [arXiv:hep-ph/0306107 [hep-ph]].
66. J. Heinonen, R. J. Hill and M. P. Solon, Phys. Rev. D **86**, 094020 (2012) doi:10.1103/PhysRevD.86.094020 [arXiv:1208.0601 [hep-ph]].
67. M. Berwein, N. Brambilla, S. Hwang and A. Vairo, Phys. Rev. D **99**, no.9, 094008 (2019) doi:10.1103/PhysRevD.99.094008 [arXiv:1811.05184 [hep-th]].
68. A. Pineda and J. Soto, Phys. Lett. B **495**, 323-328 (2000) doi:10.1016/S0370-2693(00)01261-2 [arXiv:hep-ph/0007197 [hep-ph]].
69. N. Brambilla, X. Garcia Tormo, i, J. Soto and A. Vairo, Phys. Lett. B **647**, 185-193 (2007) doi:10.1016/j.physletb.2007.02.015 [arXiv:hep-ph/0610143 [hep-ph]].

70. N. Brambilla, A. Vairo, X. Garcia Tormo, i and J. Soto, Phys. Rev. D **80**, 034016 (2009) doi:10.1103/PhysRevD.80.034016 [arXiv:0906.1390 [hep-ph]].
71. A. Bazavov, N. Brambilla, X. Garcia Tormo, i, P. Petreczky, J. Soto and A. Vairo, Phys. Rev. D **86**, 114031 (2012) doi:10.1103/PhysRevD.86.114031 [arXiv:1205.6155 [hep-ph]].
72. C. Ayala, X. Lobregat and A. Pineda, JHEP **09**, 016 (2020) doi:10.1007/JHEP09(2020)016 [arXiv:2005.12301 [hep-ph]].
73. C. Peset, A. Pineda and J. Segovia, JHEP **09**, 167 (2018) doi:10.1007/JHEP09(2018)167 [arXiv:1806.05197 [hep-ph]].
74. Y. Kiyo and Y. Sumino, Nucl. Phys. B **889**, 156-191 (2014) doi:10.1016/j.nuclphysb.2014.10.010 [arXiv:1408.5590 [hep-ph]].
75. H. Takaura, T. Kaneko, Y. Kiyo and Y. Sumino, JHEP **04**, 155 (2019) doi:10.1007/JHEP04(2019)155 [arXiv:1808.01643 [hep-ph]].
76. A. Pineda, Prog. Part. Nucl. Phys. **67**, 735-785 (2012) doi:10.1016/j.pnpnp.2012.01.038 [arXiv:1111.0165 [hep-ph]].
77. B. A. Kniehl, A. A. Penin, Y. Schroder, V. A. Smirnov and M. Steinhauser, Phys. Lett. B **607**, 96-100 (2005) doi:10.1016/j.physletb.2004.12.024 [arXiv:hep-ph/0412083 [hep-ph]].
78. N. Brambilla, A. Pineda, J. Soto and A. Vairo, Phys. Lett. B **470**, 215 (1999) doi:10.1016/S0370-2693(99)01301-5 [arXiv:hep-ph/9910238 [hep-ph]].
79. B. A. Kniehl, A. A. Penin, V. A. Smirnov and M. Steinhauser, Nucl. Phys. B **635**, 357-383 (2002) doi:10.1016/S0550-3213(02)00403-0 [arXiv:hep-ph/0203166 [hep-ph]].
80. K. J. Juge, J. Kuti and C. Morningstar, Phys. Rev. Lett. **90**, 161601 (2003) doi:10.1103/PhysRevLett.90.161601 [arXiv:hep-lat/0207004 [hep-lat]].
81. G. S. Bali and A. Pineda, Phys. Rev. D **69**, 094001 (2004) doi:10.1103/PhysRevD.69.094001 [arXiv:hep-ph/0310130 [hep-ph]].
82. G. S. Bali, K. Schilling and A. Wachter, Phys. Rev. D **56**, 2566-2589 (1997) doi:10.1103/PhysRevD.56.2566 [arXiv:hep-lat/9703019 [hep-lat]].
83. Y. Koma, M. Koma and H. Wittig, Phys. Rev. Lett. **97**, 122003 (2006) doi:10.1103/PhysRevLett.97.122003 [arXiv:hep-lat/0607009 [hep-lat]].
84. Y. Koma, M. Koma and H. Wittig, PoS **LATTICE2007**, 111 (2007) doi:10.22323/1.042.0111 [arXiv:0711.2322 [hep-lat]].
85. L. Müller, O. Philipsen, C. Reisinger and M. Wagner, Phys. Rev. D **100**, no.5, 054503 (2019) doi:10.1103/PhysRevD.100.054503 [arXiv:1907.01482 [hep-lat]].
86. A. Bazavov *et al.* [TUMQCD], Phys. Rev. D **100**, no.11, 114511 (2019) doi:10.1103/PhysRevD.100.114511 [arXiv:1907.11747 [hep-lat]].
87. N. Brambilla, Y. Sumino and A. Vairo, Phys. Rev. D **65**, 034001 (2002) doi:10.1103/PhysRevD.65.034001 [arXiv:hep-ph/0108084 [hep-ph]].
88. N. Brambilla, Y. Jia and A. Vairo, Phys. Rev. D **73**, 054005 (2006) doi:10.1103/PhysRevD.73.054005 [arXiv:hep-ph/0512369 [hep-ph]].
89. N. Brambilla, P. Pietrulewicz and A. Vairo, Phys. Rev. D **85**, 094005 (2012) doi:10.1103/PhysRevD.85.094005 [arXiv:1203.3020 [hep-ph]].
90. A. Pineda and J. Segovia, Phys. Rev. D **87**, no.7, 074024 (2013) doi:10.1103/PhysRevD.87.074024 [arXiv:1302.3528 [hep-ph]].
91. J. Segovia, S. Steinbeißer and A. Vairo, Phys. Rev. D **99**, no.7, 074011 (2019) doi:10.1103/PhysRevD.99.074011 [arXiv:1811.07590 [hep-ph]].
92. N. Brambilla and A. Vairo, Phys. Rev. D **71**, 034020 (2005) doi:10.1103/PhysRevD.71.034020 [arXiv:hep-ph/0411156 [hep-ph]].
93. N. Brambilla, D. Eiras, A. Pineda, J. Soto and A. Vairo, Phys. Rev. D **67**, 034018 (2003) doi:10.1103/PhysRevD.67.034018 [arXiv:hep-ph/0208019 [hep-ph]].
94. N. Brambilla and A. Vairo, Phys. Rev. D **62**, 094019 (2000) doi:10.1103/PhysRevD.62.094019 [arXiv:hep-ph/0002075 [hep-ph]].
95. C. Peset, A. Pineda and M. Stahlhofen, JHEP **05**, 017 (2016) doi:10.1007/JHEP05(2016)017 [arXiv:1511.08210 [hep-ph]].
96. N. Brambilla, A. Vairo and T. Rosch, Phys. Rev. D **72**, 034021 (2005) doi:10.1103/PhysRevD.72.034021 [arXiv:hep-ph/0506065 [hep-ph]].

97. N. Brambilla, J. Ghiglieri and A. Vairo, Phys. Rev. D **81**, 054031 (2010) doi:10.1103/PhysRevD.81.054031 [arXiv:0911.3541 [hep-ph]].
98. T. T. Takahashi, H. Matsufuru, Y. Nemoto and H. Suganuma, Phys. Rev. Lett. **86**, 18-21 (2001) doi:10.1103/PhysRevLett.86.18 [arXiv:hep-lat/0006005 [hep-lat]].
99. T. T. Takahashi, H. Suganuma, Y. Nemoto and H. Matsufuru, Phys. Rev. D **65**, 114509 (2002) doi:10.1103/PhysRevD.65.114509 [arXiv:hep-lat/0204011 [hep-lat]].
100. G. S. Bali, K. Schilling and C. Schlichter, Phys. Rev. D **51**, 5165-5198 (1995) doi:10.1103/PhysRevD.51.5165 [arXiv:hep-lat/9409005 [hep-lat]].
101. P. Bicudo, N. Cardoso and M. Cardoso, Phys. Rev. D **98**, no.11, 114507 (2018) doi:10.1103/PhysRevD.98.114507 [arXiv:1808.08815 [hep-lat]].
102. R. Yanagihara and M. Kitazawa, PTEP **2019**, no.9, 093B02 (2019) [erratum: PTEP **2020**, no.7, 079201 (2020)] doi:10.1093/ptep/ptz093 [arXiv:1905.10056 [hep-ph]].
103. M. Baker, V. Chelnokov, L. Cosmai, F. Cuteri and A. Papa, [arXiv:2111.06618 [hep-lat]].
104. J. Greensite, Prog. Part. Nucl. Phys. **51**, 1 (2003) doi:10.1016/S0146-6410(03)90012-3 [arXiv:hep-lat/0301023 [hep-lat]].
105. M. Baker, J. S. Ball and F. Zachariasen, Phys. Rept. **209**, 73-127 (1991) doi:10.1016/0370-1573(91)90123-4
106. N. Isgur and J. E. Paton, Phys. Rev. D **31**, 2910 (1985) doi:10.1103/PhysRevD.31.2910
107. H. G. Dosch and Y. A. Simonov, Phys. Lett. B **205**, 339-344 (1988) doi:10.1016/0370-2693(88)91675-9
108. M. Baker, J. S. Ball, N. Brambilla, G. M. Prosperi and F. Zachariasen, Phys. Rev. D **54**, 2829-2844 (1996) [erratum: Phys. Rev. D **56**, 2475 (1997)] doi:10.1103/PhysRevD.56.2475 [arXiv:hep-ph/9602419 [hep-ph]].
109. M. Baker, N. Brambilla, H. G. Dosch and A. Vairo, Phys. Rev. D **58**, 034010 (1998) doi:10.1103/PhysRevD.58.034010 [arXiv:hep-ph/9802273 [hep-ph]].
110. N. Brambilla, M. Groher, H. E. Martinez and A. Vairo, Phys. Rev. D **90**, no.11, 114032 (2014) doi:10.1103/PhysRevD.90.114032 [arXiv:1407.7761 [hep-ph]].
111. G. Perez-Nadal and J. Soto, Phys. Rev. D **79**, 114002 (2009) doi:10.1103/PhysRevD.79.114002 [arXiv:0811.2762 [hep-ph]].
112. N. Brambilla and A. Vairo, Phys. Rev. D **55**, 3974-3986 (1997) doi:10.1103/PhysRevD.55.3974 [arXiv:hep-ph/9606344 [hep-ph]].
113. K. Nawa, H. Suganuma and T. Kojo, Phys. Rev. D **75**, 086003 (2007) doi:10.1103/PhysRevD.75.086003 [arXiv:hep-th/0612187 [hep-th]].
114. K. Amemiya and H. Suganuma, Phys. Rev. D **60**, 114509 (1999) doi:10.1103/PhysRevD.60.114509 [arXiv:hep-lat/9811035 [hep-lat]].
115. S. Sasaki, H. Suganuma and H. Toki, Prog. Theor. Phys. **94**, 373-384 (1995) doi:10.1143/PTP.94.373
116. J. Soto and J. Tarrús Castellà, Phys. Rev. D **104**, 074027 (2021) doi:10.1103/PhysRevD.104.074027 [arXiv:2108.00496 [hep-ph]].
117. N. Brambilla, V. Leino, O. Philipsen, C. Reisinger, A. Vairo and M. Wagner, [arXiv:2106.01794 [hep-lat]].
118. A. Vairo, Mod. Phys. Lett. A **31**, no.34, 1630039 (2016) doi:10.1142/S0217732316300391
119. N. Brambilla, H. S. Chung and A. Vairo, JHEP **09**, 032 (2021) [arXiv:2106.09417 [hep-ph]].
120. N. Brambilla, H. S. Chung and A. Vairo, Phys. Rev. Lett. **126**, no.8, 082003 (2021) doi:10.1103/PhysRevLett.126.082003 [arXiv:2007.07613 [hep-ph]].
121. N. Brambilla, H. S. Chung, D. Müller and A. Vairo, JHEP **04**, 095 (2020) doi:10.1007/JHEP04(2020)095 [arXiv:2002.07462 [hep-ph]]. Copy to ClipboardDownload
122. N. Brambilla, [arXiv:2111.10788 [hep-lat]].
123. N. Brambilla, S. Eidelman, C. Hanhart, A. Nefediev, C. P. Shen, C. E. Thomas, A. Vairo and C. Z. Yuan, Phys. Rept. **873**, 1-154 (2020) doi:10.1016/j.physrep.2020.05.001 [arXiv:1907.07583 [hep-ex]].
124. M. Tanabashi *et al.* [Particle Data Group], Phys. Rev. D **98** (2018) no.3, 030001.
125. S. K. Choi *et al.* [Belle], Phys. Rev. Lett. **91** (2003), 262001.
126. A. Ali, J. S. Lange and S. Stone, Prog. Part. Nucl. Phys. **97** (2017), 123-198.

127. F. K. Guo, C. Hanhart, U. G. Meißner, Q. Wang, Q. Zhao and B. S. Zou, *Rev. Mod. Phys.* **90** (2018) no.1, 015004.
128. M. T. AlFiky, F. Gabbiani and A. A. Petrov, *Phys. Lett. B* **640** (2006), 238-245 doi:10.1016/j.physletb.2006.07.069 [arXiv:hep-ph/0506141 [hep-ph]].
129. E. Braaten and M. Lu, *Phys. Rev. D* **76** (2007), 094028.
130. E. Braaten and M. Kusunoki, *Phys. Rev. D* **69** (2004), 074005.
131. S. Fleming and T. Mehen, *Phys. Rev. D* **85** (2012), 014016.
132. E. Braaten, C. Langmack and D. H. Smith, *Phys. Rev. D* **90** (2014) no.1, 014044.
133. E. Braaten, C. Langmack and D. H. Smith, *Phys. Rev. Lett.* **112** (2014), 222001.
134. G. Chiladze, A. F. Falk and A. A. Petrov, *Phys. Rev. D* **58** (1998), 034013 doi:10.1103/PhysRevD.58.034013 [arXiv:hep-ph/9804248 [hep-ph]].
135. A. A. Petrov, *J. Phys. Conf. Ser.* **9** (2005), 83-86 doi:10.1088/1742-6596/9/1/013
136. M. Berwein, N. Brambilla, J. Tarrús Castellà and A. Vairo, *Phys. Rev. D* **92** (2015) no.11, 114019.
137. N. Brambilla, G. Krein, J. Tarrús Castellà and A. Vairo, *Phys. Rev. D* **97** (2018) no.1, 016016.
138. N. Brambilla, W. K. Lai, J. Segovia and J. Tarrús Castellà, *Phys. Rev. D* **101** (2020) no.5, 054040.
139. N. Brambilla, W. K. Lai, J. Segovia, J. Tarrús Castellà and A. Vairo, *Phys. Rev. D* **99** (2019) no.1, 014017.
140. J. Soto and J. Tarrús Castellà, *Phys. Rev. D* **102** (2020) no.1, 014012.
141. R. Oncala and J. Soto, *Phys. Rev. D* **96** (2017) no.1, 014004.
142. S. Borsanyi, Z. Fodor, J. N. Guenther, R. Kara, S. D. Katz, P. Parotto, A. Pasztor, C. Ratti and K. K. Szabo, *Phys. Rev. Lett.* **125**, no.5, 052001 (2020) doi:10.1103/PhysRevLett.125.052001 [arXiv:2002.02821 [hep-lat]].
143. T. Matsui and H. Satz, *Phys. Lett. B* **178**, 416-422 (1986) doi:10.1016/0370-2693(86)91404-8
144. E. Braaten and R. D. Pisarski, *Nucl. Phys. B* **337**, 569-634 (1990) doi:10.1016/0550-3213(90)90508-B
145. E. Braaten and R. D. Pisarski, *Phys. Rev. D* **45**, no.6, R1827 (1992) doi:10.1103/PhysRevD.45.R1827
146. M. Laine, O. Philipsen, P. Romatschke and M. Tassler, *JHEP* **03**, 054 (2007) doi:10.1088/1126-6708/2007/03/054 [arXiv:hep-ph/0611300 [hep-ph]].
147. N. Brambilla, *PoS HardProbes2020* (2021), 017.
148. N. Brambilla, J. Ghiglieri, A. Vairo and P. Petreczky, *Phys. Rev. D* **78**, 014017 (2008) doi:10.1103/PhysRevD.78.014017 [arXiv:0804.0993 [hep-ph]].
149. N. Brambilla, M. A. Escobedo, J. Ghiglieri, J. Soto and A. Vairo, *JHEP* **09**, 038 (2010) doi:10.1007/JHEP09(2010)038 [arXiv:1007.4156 [hep-ph]].
150. N. Brambilla, M. A. Escobedo, J. Ghiglieri and A. Vairo, *JHEP* **12**, 116 (2011) doi:10.1007/JHEP12(2011)116 [arXiv:1109.5826 [hep-ph]].
151. N. Brambilla, M. A. Escobedo, J. Ghiglieri and A. Vairo, *JHEP* **05**, 130 (2013) doi:10.1007/JHEP05(2013)130 [arXiv:1303.6097 [hep-ph]].
152. M. A. Escobedo and J. Soto, *Phys. Rev. A* **78**, 032520 (2008) doi:10.1103/PhysRevA.78.032520 [arXiv:0804.0691 [hep-ph]].
153. G. Aarts, C. Allton, S. Kim, M. P. Lombardo, M. B. Oktay, S. M. Ryan, D. K. Sinclair and J. I. Skullerud, *JHEP* **11**, 103 (2011) doi:10.1007/JHEP11(2011)103 [arXiv:1109.4496 [hep-lat]].
154. A. Rothkopf, T. Hatsuda and S. Sasaki, *Phys. Rev. Lett.* **108**, 162001 (2012) doi:10.1103/PhysRevLett.108.162001 [arXiv:1108.1579 [hep-lat]].
155. A. Rothkopf, *Phys. Rept.* **858**, 1-117 (2020) doi:10.1016/j.physrep.2020.02.006 [arXiv:1912.02253 [hep-ph]].
156. D. Bala, O. Kaczmarek, R. Larsen, S. Mukherjee, G. Parkar, P. Petreczky, A. Rothkopf and J. H. Weber, [arXiv:2110.11659 [hep-lat]].
157. J. Ghiglieri, A. Kurkela, M. Strickland and A. Vuorinen, *Phys. Rept.* **880** (2020), 1-73 [arXiv:2002.10188 [hep-ph]].

158. M. Berwein, N. Brambilla, P. Petreczky and A. Vairo, Phys. Rev. D **96** (2017) no.1, 014025 [arXiv:1704.07266 [hep-ph]].
159. M. Berwein, N. Brambilla, P. Petreczky and A. Vairo, Phys. Rev. D **93** (2016) no.3, 034010 [arXiv:1512.08443 [hep-ph]].
160. N. Brambilla, J. Ghiglieri, P. Petreczky and A. Vairo, Phys. Rev. D **82** (2010), 074019 [arXiv:1007.5172 [hep-ph]].
161. A. Bazavov *et al.* [TUMQCD], Phys. Rev. D **98** (2018) no.5, 054511 [arXiv:1804.10600 [hep-lat]].
162. A. Bazavov, N. Brambilla, H. T. Ding, P. Petreczky, H. P. Schadler, A. Vairo and J. H. Weber, Phys. Rev. D **93** (2016) no.11, 114502 [arXiv:1603.06637 [hep-lat]].
163. A. Bazavov and J. H. Weber, Prog. Part. Nucl. Phys. **116**, 103823 (2021) doi:10.1016/j.pnpnp.2020.103823 [arXiv:2010.01873 [hep-lat]].
164. N. Brambilla, M. A. Escobedo, J. Soto and A. Vairo, Phys. Rev. D **97** (2018) no.7, 074009 [arXiv:1711.04515 [hep-ph]].
165. N. Brambilla, M. A. Escobedo, J. Soto and A. Vairo, Phys. Rev. D **96** (2017) no.3, 034021 [arXiv:1612.07248 [hep-ph]].
166. N. Brambilla, M. A. Escobedo, A. Vairo and P. Vander Griend, Phys. Rev. D **100** (2019) no.5, 054025 [arXiv:1903.08063 [hep-ph]].
167. N. Brambilla, M. Á. Escobedo, M. Strickland, A. Vairo, P. Vander Griend and J. H. Weber, Phys. Rev. D **104**, no.9, 094049 (2021) [arXiv:2107.06222 [hep-ph]].
168. N. Brambilla, M. Á. Escobedo, M. Strickland, A. Vairo, P. Vander Griend and J. H. Weber, JHEP **05**, 136 (2021) [arXiv:2012.01240 [hep-ph]].
169. H. B. Omar, M. Á. Escobedo, A. Islam, M. Strickland, S. Thapa, P. Vander Griend and J. H. Weber, Comput. Phys. Commun. **273**, 108266 (2022) doi:10.1016/j.cpc.2021.108266 [arXiv:2107.06147 [physics.comp-ph]].
170. M. Á. Escobedo, Phys. Rev. D **103**, no.3, 034010 (2021) doi:10.1103/PhysRevD.103.034010 [arXiv:2010.10424 [hep-ph]].
171. Y. Akamatsu, Prog. Part. Nucl. Phys. **123**, 103932 (2022) doi:10.1016/j.pnpnp.2021.103932 [arXiv:2009.10559 [nucl-th]].
172. Y. Akamatsu, Phys. Rev. D **91**, no.5, 056002 (2015) doi:10.1103/PhysRevD.91.056002 [arXiv:1403.5783 [hep-ph]].
173. X. Yao, W. Ke, Y. Xu, S. A. Bass, T. Mehen and B. Müller, [arXiv:2002.04079 [hep-ph]]; X. Yao and T. Mehen, [arXiv:2009.02408 [hep-ph]].
174. X. Yao and T. Mehen, Phys. Rev. D **99** (2019) no.9, 096028 [arXiv:1811.07027 [hep-ph]].
175. X. Yao, Int. J. Mod. Phys. A **36**, no.20, 2130010 (2021) doi:10.1142/S0217751X21300106 [arXiv:2102.01736 [hep-ph]].
176. R. Sharma and A. Tiwari, Phys. Rev. D **101** (2020) no.7, 074004 [arXiv:1912.07036 [hep-ph]].
177. N. Brambilla, V. Leino, P. Petreczky and A. Vairo, Phys. Rev. D **102**, no.7, 074503 (2020) doi:10.1103/PhysRevD.102.074503 [arXiv:2007.10078 [hep-lat]].
178. S. Acharya *et al.* [ALICE], Phys. Lett. B **822**, 136579 (2021) doi:10.1016/j.physletb.2021.136579 [arXiv:2011.05758 [nucl-ex]].
179. A. M. Sirunyan *et al.* [CMS], Phys. Lett. B **790**, 270-293 (2019) doi:10.1016/j.physletb.2019.01.006 [arXiv:1805.09215 [hep-ex]].
180. Songkyo Lee (ATLAS Collaboration) Quark Matter 2020 <https://indico.cern.ch/event/792436/contributions/3535775/>
181. N. Brambilla, V. Shtabovenko, J. Tarrús Castellà and A. Vairo, Phys. Rev. D **95**, no.11, 116004 (2017) doi:10.1103/PhysRevD.95.116004 [arXiv:1704.03476 [hep-ph]].

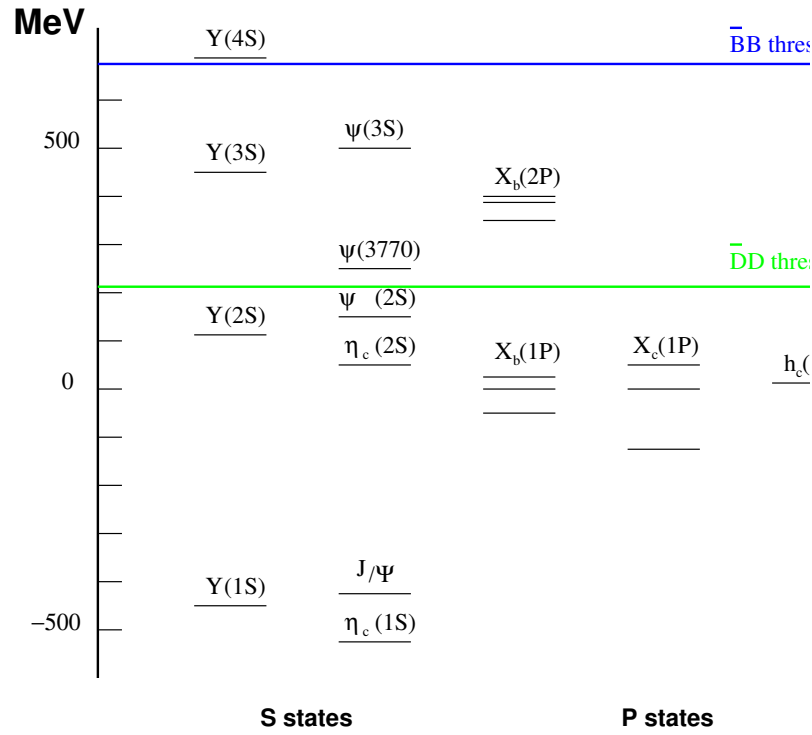


Fig. 1 The experimental quarkonium energy levels ($b\bar{b}$ and $c\bar{c}$) as known in the eighties (plotted as relative to the spin-average of the $\chi_b(1P)$ and $\chi_c(1P)$ states to be able to present the two sectors in the same plot). The states are identified by names and mass in parenthesis, Υ being the vector states (with $L = 0$) in bottomonium, J/ψ and ψ the vector states in charmonium sector, η the pseudoscalar states and χ and h states with $L = 1$ and different total angular momentum. The first strong decay thresholds are also shown.

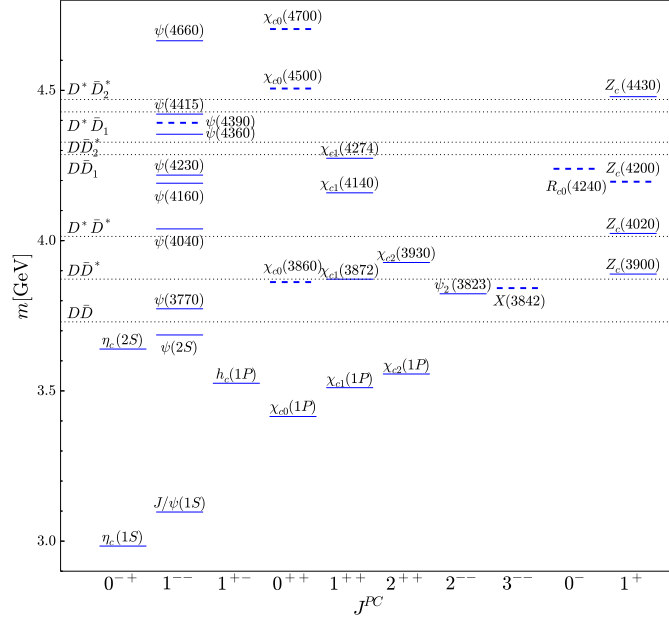


Fig. 2 The spectrum of states in the $c\bar{c}$ sector as of 2019, taken from ref. [123]. Thin solid lines represent the states established experimentally and dashed lines are for those that are claimed but not (yet) established (a state is regarded as established if it is seen in different modes). States whose quantum numbers are undetermined are not shown. States in the plot are labeled according to the PDG primary naming scheme that superseded the X Y Z notation, for further details see [123]. Dashed lines show some relevant thresholds that open in the considered mass range; here D_1 stands for $D_1(2420)$ and D_2^* for $D_2^*(2460)$. Thresholds with hidden strangeness or involving broad states are not shown. The states shown in the two columns to the right are isovectors containing a $\bar{c}c$ pair; they are necessarily exotic. The just discovered state $X(6900)$ [38] made by two charm and two anticharm quarks would be out of the scale of the figure. More states have been observed after 2019.

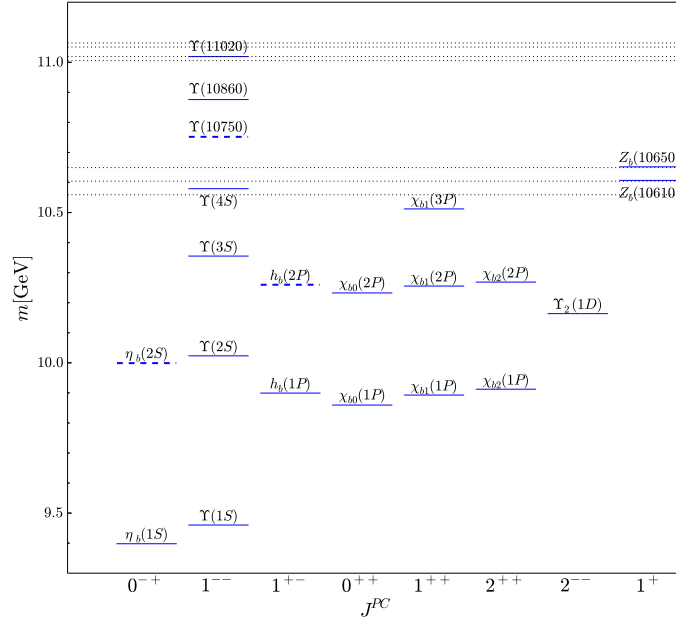


Fig. 3 The spectrum of states in the $\bar{c}c$ sector as of 2019, taken from ref. [123]. Thin solid lines represent the states established experimentally and dashed lines are for those that are claimed but not (yet) established (a state is regarded as established if it is seen in different modes). States whose quantum numbers are undetermined are not shown. States in the plot are labeled according to the PDG primary naming scheme that superseded the X Y Z notation, for further details see [123]. Dashed lines show some relevant thresholds that open in the considered mass range; here D_1 stands for $D_1(2420)$ and D_2^* for $D_2^*(2460)$. Thresholds with hidden strangeness or involving broad states are not shown. The states shown in the two columns to the right are isovectors containing a $\bar{c}c$ pair; they are necessarily exotic.

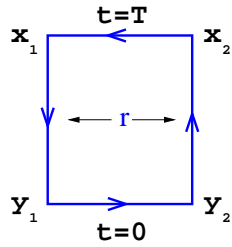


Fig. 4 The static Wilson loop. It contains the interaction of a static quark-antiquark pair created at a time $t = 0$ and annihilated at a subsequent large time T . Initial and final states are made gauge invariant by the presence of Schwinger line given in eq. (5).

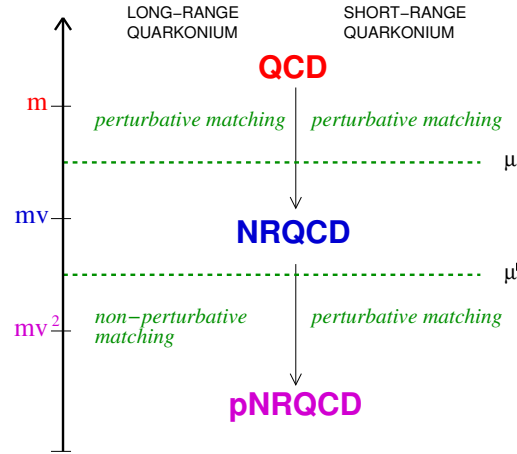


Fig. 5 The hard, soft and ultrasoft scales of quarkonium and the corresponding NREFTs that can be constructed. NRQCD follows from the integration of the gluons and quarks at the hard scale, pNRQCD follows from integration of gluons at the soft scale. If the soft scale is bigger than Λ_{QCD} then the matching from NRQCD to pNRQCD is perturbative, otherwise it is nonperturbative.

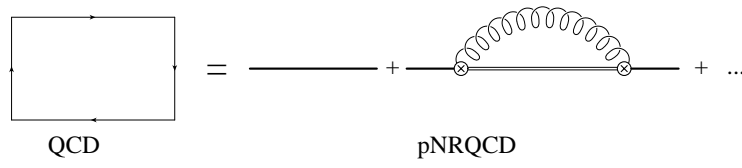


Fig. 6 The matching of the static potential. On the right side are the pNRQCD fields: simple lines are singlet propagator, double lines are octet propagators, circled-crosses are the singlet-octet vertices of Eq. (19) and the wavy line is the US gluon propagator.

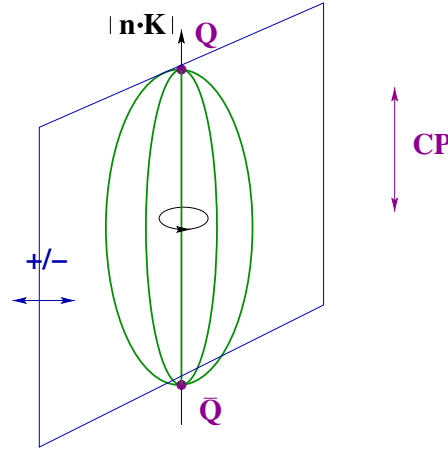


Fig. 7 Quarkonium hybrid symmetries.

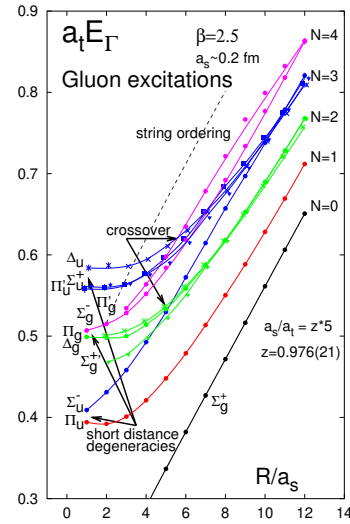


Fig. 8 Hybrid static energies, E_T , in lattice units, from [80].

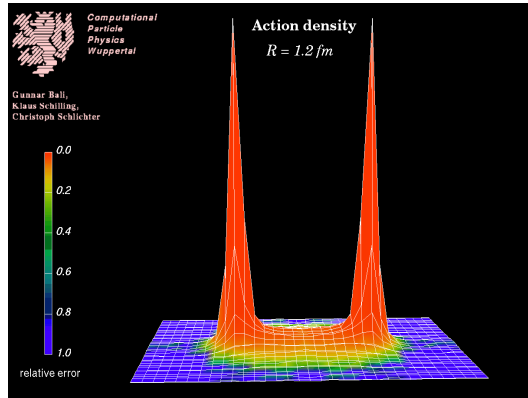


Fig. 9 The origin of the linear potential between the static quark and antiquark may be traced back to a flux tube: a string of gluon energy between the quark pair. Here we present the hystorical picture of the action density distribution between a static quark antiquark couple in $SU(2)$ at a physical distance of 1.2 fm, from [100].

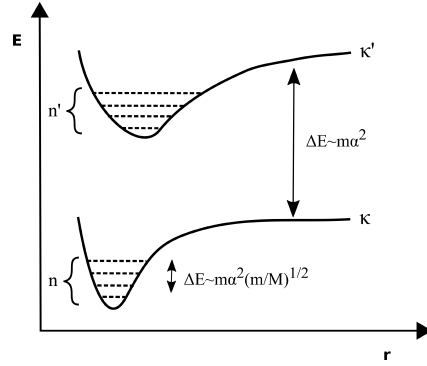


Fig. 10 Pictorial view of electronic static energies in QED, labelled by a collective quantum number κ .

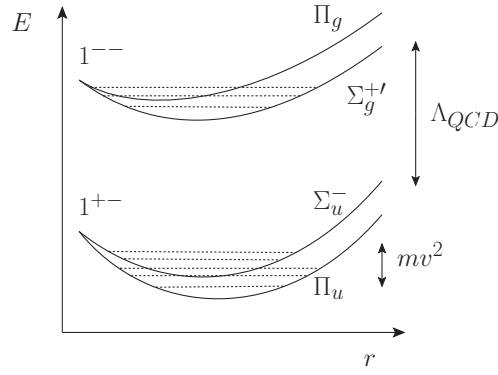


Fig. 11 Pictorial view of the gluonic (or hybrid) static energies, E_G , in QCD. The collective quantum number κ has been detailed in Λ_η^σ as explained in the section on strongly coupled pNRQCD. It corresponds to the actual lattice results in Fig. 8.

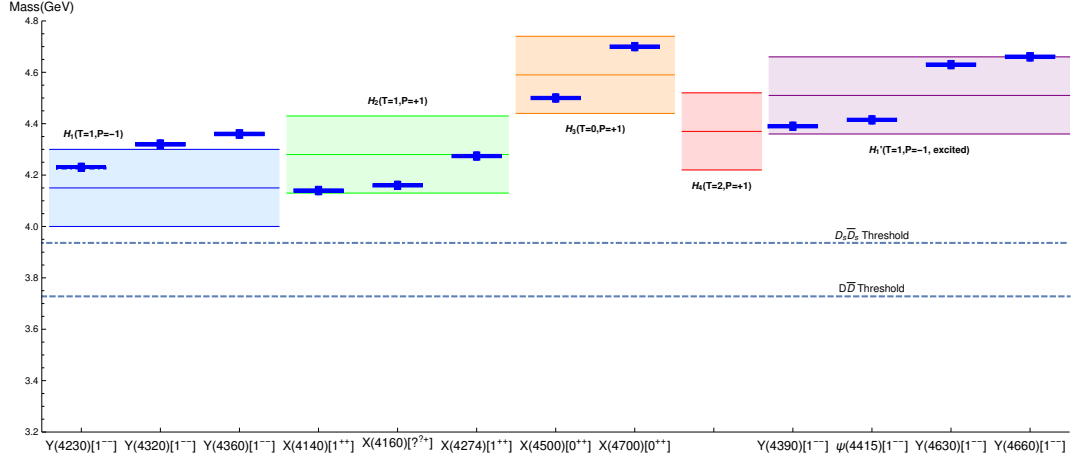


Fig. 12 Mass spectrum of neutral exotic charmonium states obtained by solving the BOEFT coupled Schrödinger equations. The neutral experimental states that have matching quantum numbers are plotted in solid blue lines. In the figure T stay for the total angular momentum. H'_1 is the first H_1 radial excitation of H_1 . The multiplets have been plotted with error bands corresponding to a gluelump mass uncertainty of 0.15 GeV. Figure taken from [123].

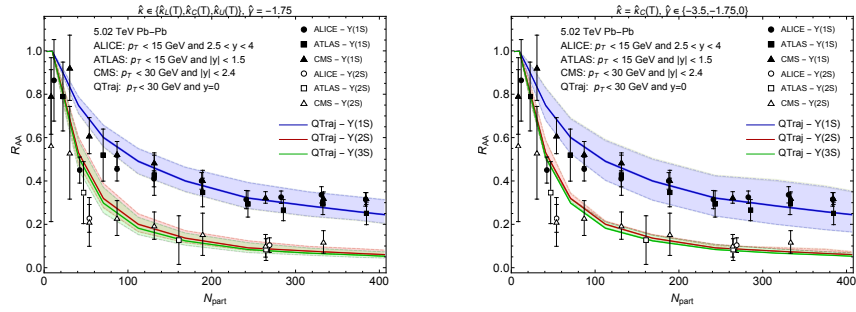


Fig. 13 The nuclear modification factor R_{AA} of the $Y(1S)$, $Y(2S)$, and $Y(3S)$ as a function of N_{part} compared to experimental measurements from the ALICE [178], ATLAS [180], and CMS [179] collaborations. The bands in the theoretical curves indicate variation with respect to $\hat{\kappa}(T)$ (left) and $\hat{\gamma}$ (right). The central curves represent the central values of $\hat{\kappa}(T)$ and $\hat{\gamma}$, and the dashed and dot-dashed lines represent the lower and upper values, respectively, of $\hat{\kappa}(T) \equiv \kappa/T^3$ and $\hat{\gamma} \equiv \gamma/T^3$, see text for the definition of these parameters. Figure taken from [167].